AECL EACL

AECL-11496, COG-95-561-I

Verification of the MOTIF Code Version 3.0

Vérification du code de calcul MOTIF, version 3.0

T. Chan, V. Guvanasen, B.W. Nakka, J.A.K. Reid,
N.W. Scheier, F.W. Stanchell

December 1996 décembre

AECL EACL

VERIFICATION OF THE MOTIF CODE VERSION 3.0

by

T. Chan, V. Guvanasen, B.W. Nakka,
J.A.K. Reid, N.W. Scheier and F.W. Stanchell

Whiteshell Laboratories
Pinawa, Manitoba R0E 1L0
1996

AECL-11496
COG-95-561-I

VERIFICATION OF THE MOTIF CODE VERSION 3.0

by

T. Chan, V. Guvanasen, B.W. Nakka,
J.A.K. Reid, N.W. Scheier and F.W. Stanchell

ABSTRACT

As part of the Canadian Nuclear Fuel Waste Management Program (CNFWMP), AECL has developed a three-dimensional finite-element code, MOTIF (Model Of Transport In Fractured/porous media), for detailed modelling of groundwater flow, heat transport and solute transport in a fractured rock mass. The code solves the transient and steady-state equations of groundwater flow, solute (including one-species radionuclide) transport, and heat transport in variably-saturated fractured/porous media. The initial development was completed in 1985 (Guvanasen 1985) and version 3.0 was completed in 1986. This version is documented in detail in Guvanasen and Chan (in preparation).

This report describes a series of fourteen verification cases which has been used to test the numerical solution techniques and coding of MOTIF, as well as demonstrate some of the MOTIF analysis capabilities. For each case the MOTIF solution has been compared with a corresponding analytical or independently developed alternate numerical solution.

Several of the verification cases were included in Level 1 of the International Hydrologic Code Intercomparison Project (HYDROCOIN). The MOTIF results for these cases were also described in the HYDROCOIN Secretariat's compilation and comparison of results submitted by the various project teams (Swedish Nuclear Power Inspectorate 1988).

It is evident from the graphical comparisons presented that the MOTIF solutions for the fourteen verification cases are generally in excellent agreement with known analytical or numerical solutions obtained from independent sources.

This series of verification studies has established the ability of the MOTIF finite-element code to accurately model the groundwater flow and solute and heat transport phenomena for which it is intended.

Whiteshell Laboratories
Pinawa, Manitoba R0E 1L0
1996

AECL-11496
COG-95-561-I

VÉRIFICATION DU CODE DE CALCUL MOTIF, VERSION 3.0

par

T. Chan, V. Guvanasen, B.W. Nakka,
J.A.K. Reid, N.W. Scheier et F.W. Stanchell

RÉSUMÉ

Dans le cadre du Programme canadien de gestion des déchets de combustible nucléaire (PCGDCN), EACL a mis au point un code de calcul par éléments finis tridimensionnel, nommé MOTIF (*Model Of Transport In Fractured/porous media* (modèle de transport en milieux fracturés ou poreux)), destiné à la modélisation précise de l'écoulement des eaux souterraines, du transport de la chaleur et du transport des solutés dans un massif rocheux fracturé. Le code de calcul permet de résoudre les équations de l'état transitoire et de l'état stable de l'écoulement des eaux souterraines, du transport des solutés (y compris les radionucléides à espèce unique) et du transport de la chaleur dans les milieux fracturés ou poreux saturés de façon variable. L'élaboration de la première version a été achevée en 1985 (Guvanasen 1985), et la version 3.0 en 1986. Guvanasen et Chan ont rédigé une documentation détaillée sur cette version (en préparation).

Le présent rapport donne une description d'une série de quatorze cas de vérification qui ont été utilisés pour mettre à l'épreuve les techniques de solution numérique et le programme de MOTIF ainsi que pour faire une démonstration de quelques-unes des fonctions d'analyse de ce dernier. Dans chaque cas, la solution donnée par MOTIF a été comparée à une solution analytique équivalente ou à une autre solution numérique calculée de façon indépendante.

Plusieurs de ces cas de vérification ont été incorporés au niveau 1 du Projet international d'intercomparaison des codes de calcul hydrogéologiques (*Hydrogeologic Code Intercomparison Project*) (HYDROCOIN). Les résultats produits par MOTIF dans ces mêmes cas ont aussi été présentés dans le document établi par le secrétariat du Projet HYDROCOIN et qui fait la compilation et la comparaison des résultats soumis par les divers groupes de projet (*Swedish Nuclear Power Inspectorate* 1988).

Il ressort clairement des comparaisons graphiques qui sont présentées que les solutions données par MOTIF dans ces quatorze cas de vérification concordent en général extrêmement bien avec les solutions numériques ou analytiques connues provenant de sources indépendantes.

Cette série d'études de vérification a permis d'établir que le code de calcul par éléments finis MOTIF modélise avec précision les phénomènes d'écoulement des eaux souterraines et de transport de la chaleur et des solutés pour lesquels il est prévu.

Laboratoires de Whiteshell
Pinawa (Manitoba) R0E 1L0
1996

AECL-11496
COG-95-561-I

CONTENTS

continued...

CONTENTS (concluded)

LIST OF TABLES

LIST OF FIGURES

continued...

LIST OF FIGURES (concluded)

1. INTRODUCTION

As part of the Canadian Nuclear Fuel Waste Management Program (CNFWMP), AECL has developed a three-dimensional finite-element code, MOTIF (Model Of Transport In Fractured/ porous media), for detailed modelling of groundwater flow, heat transport and solute transport in a fractured rock mass. The code solves the transient and steady-state equations of groundwater flow, solute (including one-species radionuclide) transport, and heat transport in variably-saturated fractured/porous media. The initial development was completed in 1985 (Guvanasen 1985) and version 3.0 was completed in 1986. This version is documented in detail in Guvanasen and Chan (in preparation).

This report describes a series of fourteen verification cases which has been used to test the numerical solution techniques and coding of MOTIF, as well as demonstrate some of the MOTIF analysis capabilities. For each case the MOTIF solution has been compared with a corresponding analytical or independently developed alternate numerical solution.

The verification cases included in this report are:

CASE 1: Steady-state groundwater flow in a rock mass containing intersecting fracture zones

CASE 2: A groundwater withdrawal well in a confined horizontal aquifer intersected by a vertical fracture

CASE 3: Transient groundwater flow from a borehole in a permeable medium underlain by a horizontal fracture

CASE 4: One-dimensional solute transport in a semi-infinite porous medium

CASE 5: One-dimensional solute transport in a finite porous medium

CASE 6: Solute transport along a discrete fracture with diffusion into the background rock mass

CASE 7: Two-dimensional steady state groundwater flow and solute transport in an unconfined aquifer

CASE 8: Fully coupled fluid flow and heat transport

CASE 9: Fully coupled fluid flow and solute transport

CASE 10: Rise of groundwater mound due to infiltration from a strip recharge pit

CASE 11: Drainage of water from a sand column

CASE 12: Steady-state dipolar groundwater flow in a confined aquifer

CASE 13: Solute transport in a dipolar groundwater flow field in a confined aquifer

CASE 14: The Henry Problem - Fully coupled fluid flow and solute transport.

Cases 1, 3 and 8 were included in Level 1 of the International Hydrologic Code Intercomparison Project (HYDROCOIN). The MOTIF results for these cases were also included in the HYDROCOIN Secretariat's compilation and comparison of results submitted by the various project teams (Swedish Nuclear Power Inspectorate 1988). Results for Cases 1, 3, 6, 8 and 9 were also published in Chan et al. (1987).

2. VERIFICATION CASES

2.1 CASE 1: STEADY-STATE GROUNDWATER FLOW IN A ROCK MASS CONTAINING INTERSECTING FRACTURE ZONES

This case deals with topographically driven, steady-state groundwater flow in a saturated, confined, vertical, two-dimensional porous medium containing two intersecting, thin fracture zones having a relatively high permeability compared to that of the surrounding background rock mass (Figure 1). This is the HYDROCOIN Level 1 Case 2. The background rock mass and the fracture zones are each homogeneous and isotropic.

The hydraulic head distribution in the background rock mass and fracture zones can be described by the equation:

$$\frac{\partial}{\partial x}\left(K\frac{\partial h}{\partial x}\right)+\frac{\partial}{\partial z}\left(K\frac{\partial h}{\partial z}\right)=0 \qquad \textbf{(1.1)}$$

where: h = hydraulic head
K = hydraulic conductivity
x, z = Cartesian coordinates.

For the top boundary the head is specified as equal to the ground surface elevation, i.e.:

$$h = z \qquad \textbf{(1.2a)}$$

The other boundaries are no-flow, i.e.:

$$\frac{\partial h}{\partial x}=0 \qquad \text{at } x = 0 \text{ and } x = 1600 \text{ m} \qquad \textbf{(1.2b)}$$

$$\frac{\partial h}{\partial z}=0 \qquad \text{at } z = -1000 \text{ m.} \qquad \textbf{(1.2c)}$$

The input parameter values used are listed in Table 1.

In the MOTIF solution the model is assumed to be 100 m thick. MOTIF solutions are calculated using three different discretizations, which are designated XSO, FSO and XSP and defined as follows:

XSO = coarse mesh with 312 solid elements only,
FSO = fine mesh with 788 solid elements only (Figure 2), and
XSP = coarse mesh with 280 solid elements (background rock mass) and 31 planar elements (fracture zones).

Discretization XSO is almost identical to XSP except for elements along the fracture zones; XSO uses solid elements while XSP uses planar elements. For the planar elements the equation for the head distribution is a version of a previous equation integrated across the thickness of the fracture zone (Guvanasen and Chan, in preparation). This approach is suitable because the hydraulic conductivity of the fracture zone is much higher than that of the background rock mass.

The head distributions calculated using the three discretizations are almost identical and are very close to those calculated by Grundfelt (1984) using the GWHRT finite-element code. The maximum difference is less than 1.5%. Figure 3 shows the calculated heads at an elevation z = -600 m.

2.2 CASE 2: A GROUNDWATER WITHDRAWAL WELL IN A CONFINED HORIZONTAL AQUIFER INTERSECTED BY A VERTICAL FRACTURE

This case deals with transient, groundwater flow in a saturated, square, confined, horizontal aquifer that is intersected by a thin vertical fracture. The fracture coincides with a line bisecting the aquifer and is parallel to the aquifer boundary. At the midpoint of the aquifer, which also coincides with the midpoint of the fracture zone, there is a fully penetrating withdrawal well. Because of symmetry, only one quadrant need be modelled (Figure 4). The aquifer and the fracture are each homogeneous and isotropic. The permeability of the fracture is much higher than that of the aquifer. It is assumed that the hydraulic gradient across the fracture is negligible.

The hydraulic head distribution in the aquifer can be described by the equation:

$$T_b\left(\frac{\partial^2 h}{\partial x^2}+\frac{\partial^2 h}{\partial y^2}\right)+\Phi_F = S_b\frac{\partial h}{\partial t} \qquad (2.1)$$

where: T_b = aquifer transmissivity
y = Cartesian coordinate
Φ_F = fluid source term
S_b = aquifer storativity
t = time.

The head distribution in the fracture can be described by the equation:

$$b_a \frac{\beta^3 \rho g}{12\mu} \frac{\partial^2 h}{\partial x^2} + T_b \left. \frac{\partial h}{\partial y} \right|_{-½}^{½} = b_a \beta \rho g c_f \frac{\partial h}{\partial t} \qquad \textbf{(2.2)}$$

where: b_a = aquifer thickness
β = fracture aperture
ρ = fluid density
g = gravitational acceleration
μ = fluid dynamic viscosity
c_f = fluid compressibility.

All boundaries of the model are no-flow, i.e.:

$$\frac{\partial h}{\partial x} = 0 \qquad \text{at } x = 0 \text{ and } x = 8 \text{ m} \qquad \textbf{(2.3a)}$$

$$\frac{\partial h}{\partial y} = 0 \qquad \text{at } y = 0 \text{ and } y = 8 \text{ m.} \qquad \textbf{(2.3b)}$$

Initially the head is uniform throughout the system, i.e.:

$$h = h_0 \qquad \text{at } t = 0 \qquad \textbf{(2.4)}$$

where: h_0 = initial head in the system.

The fluid source term is:

$$\Phi_F = -\frac{Q}{4} \qquad \text{at } x = 0, y = 0 \qquad \text{for } t > 0 \qquad \textbf{(2.5a)}$$

$$\Phi_F = 0 \qquad \text{at } (x,y) \neq (0,0) \qquad \textbf{(2.5b)}$$

where: Q = well pumping rate.

The input parameter values used are listed in Table 2.

In the MOTIF solution the aquifer is discretized using 144 rectangular elements and the fracture is discretized using 12 line elements (Figure 4). The solution time steps increase in a geometric progression from an initial value of 0.01 s to a maximum value of 1000 s with the ratio of successive time steps being 1.414 until the maximum is reached. A fully implicit time scheme is used.

An analytical solution for the head drawdown created by the well was given by Gringarten et al. (1974).

The comparison of the results calculated using the two methods is done in terms of dimensionless drawdown at the withdrawal well versus dimensionless time. Dimensionless time is defined by:

$$t^+ = \frac{T_b t}{4 S_b x_L^2} \tag{2.6}$$

where: x_L = model length.

Dimensionless drawdown is defined by:

$$\Delta h^+ = \frac{2\pi T_b (h_o - h)}{Q} \, . \tag{2.7}$$

As shown in Figure 5, the agreement is very good.

2.3 CASE 3: TRANSIENT GROUNDWATER FLOW FROM A BOREHOLE IN A PERMEABLE MEDIUM UNDERLAIN BY A HORIZONTAL FRACTURE

This case is concerned with modelling the transient flow of water from a finite radius, vertical borehole, which penetrates a saturated, permeable, finite cylindrical layer of rock that is underlain by a thin horizontal fracture. Both the layer of rock and the fracture are confined between impermeable horizontal boundaries (Figure 6). This is the HYDROCOIN Level 1 Case 1. The background rock mass and the fracture are each homogeneous and isotropic. The permeability of the fracture is much higher than that of the rock layer. It is assumed that the hydraulic gradient across the fracture is negligible. A prescribed time-dependent head is maintained in the borehole and a fixed head is maintained at a radial distance of 10 m from the centre of the borehole.

The hydraulic head distribution in the background rock mass can be described by the equation:

$$K_b \left(\frac{1}{\omega} \frac{\partial}{\partial \omega} \left(\omega \frac{\partial h}{\partial \omega} \right) + \frac{\partial^2 h}{\partial z^2} \right) = S_s \frac{\partial h}{\partial t} \tag{3.1}$$

where: K_b = hydraulic conductivity of background rock
ω = radial coordinate
S_s = specific storage of background rock mass.

The head distribution in the fracture can be described by the equation:

$$\frac{T_f}{\omega}\frac{\partial}{\partial\omega}\left(\omega\frac{\partial h}{\partial\omega}\right)+K_b\left.\frac{\partial h}{\partial z}\right|_{z=0}=S_f\frac{\partial h}{\partial t} \qquad (3.2)$$

where: T_f = fracture transmissivity
S_f = fracture storativity.

The boundary conditions on the model are:

$$\frac{\partial h}{\partial z}=0 \qquad \text{at } z=0 \text{ and } z=5 \text{ m} \qquad (3.3a)$$

$$h = 0 \qquad \text{at } \omega = 10 \text{ m} \qquad (3.3b)$$

$$h = h_a = h_\infty\,(1-e^{-10t}) \qquad \text{at } \omega = 0.1 \text{ m} \qquad \text{for } t > 0 \qquad (3.3c)$$

where: h_∞ = asymptotic value of head in the borehole.

Initially the heads are zero everywhere, i.e.:

$$h = 0 \qquad \text{at } t = 0. \qquad (3.4)$$

The input parameter values are listed in Table 3.

In the MOTIF simulation a 30° pie-shaped wedge of the cylindrical domain is discretized, using 187 solid elements for the background rock mass and 17 planar elements for the fracture (Figure 7). The solution time steps increase in a geometric progression from an initial value of 0.025 s to a maximum value of 246 s with the ratio of successive time steps being 1.0737. A fully implicit time scheme is used.

An analytical solution for the head distribution was given by Hodgkinson and Barker (1985).

The comparison of the results calculated using the two methods is done in terms of head relative to the asymptotic value in the borehole, i.e.: h/h_∞. As illustrated in Figure 8 for the values as a function of time at ω = 5.0 m (point A, Figure 6) in the fracture, the agreement is very good.

2.4 CASE 4: ONE-DIMENSIONAL SOLUTE TRANSPORT IN A SEMI-INFINITE POROUS MEDIUM

This case is concerned with the transport of a solute in a semi-infinite, one-dimensional column of saturated, homogeneous, porous media. A prescribed concentration is maintained at the inflow end of the column and the groundwater flows through the column with a constant, uniform velocity.

For transport under the influence of advection, dispersion, linear equilibrium sorption, and radioactive decay the solute concentration distribution in the column can be described by the equation:

$$D\frac{\partial^2 C}{\partial x^2} - u\frac{\partial C}{\partial x} - R\lambda C = R\frac{\partial C}{\partial t} \qquad (4.1)$$

where: D = hydrodynamic dispersion coefficient
C = solute concentration
u = average linear velocity
R = retardation factor
λ = radioactive decay constant.

The boundary conditions are:

$$C = C^* \qquad \text{at } x = 0 \quad \text{for } t > 0 \qquad (4.2a)$$

$$C = 0 \qquad \text{at } x = \infty \qquad (4.2b)$$

where: C* = source solute concentration.

Initially, the concentrations are zero everywhere, i.e.:

$$C = 0 \qquad \text{at } t = 0. \qquad (4.3)$$

Three subcases are considered:

(a) transport by advection and dispersion without sorption or decay;
(b) transport by advection and dispersion including sorption but not decay;
(c) transport by advection and dispersion including decay but not sorption.

The input parameter values used are listed in Table 4.

The MOTIF simulations consider a finite column 30 m long consisting of 30 uniform line elements. At the outflow end of the column the boundary condition is assumed to be:

$$\frac{\partial C}{\partial x} = 0 \qquad \text{at } x = 30 \text{ m}. \qquad (4.4)$$

The simulation duration is 100 000 s. Uniform 500 s solution time steps and a Crank-Nicholson time scheme are used.

An analytical solution for the concentration distribution for each subcase was given by Marino (1974).

The comparison of the results calculated using the two methods is done in terms of concentration relative to the source concentration, i.e.: C/C*. As shown in Figures 9, 10 and 11, the agreement is good, for at least the first 20 m of the column in all cases.

2.5 CASE 5: ONE-DIMENSIONAL SOLUTE TRANSPORT IN A FINITE POROUS MEDIUM

This case deals with the advective and dispersive transport of a solute in a 1000 m long, one-dimensional column of saturated, homogeneous porous media. An advective boundary condition is specified at the inflow end of the column, and the groundwater flows through the column with a constant uniform velocity.

The solute concentration distribution in the column can be described by the equation:

$$D\frac{\partial^2 C}{\partial x^2} - u\frac{\partial C}{\partial x} = \frac{\partial C}{\partial t} \qquad \textbf{(5.1)}$$

The boundary conditions are:

$$uC - D\frac{\partial C}{\partial x} = u\,C^* \quad \text{at } x = 0 \text{ m} \quad \text{for } t > 0 \qquad \textbf{(5.2a)}$$

$$\frac{\partial C}{\partial x} = 0 \quad \text{at } x = 1000 \text{ m.} \qquad \textbf{(5.2b)}$$

Initially the concentrations are zero everywhere, i.e.

$$C = 0 \quad \text{at } t = 0. \qquad \textbf{(5.3)}$$

The input parameter values used are listed in Table 5.

In the MOTIF simulation the column is discretized into 80 uniform line elements. The solution time steps increase in a geometric progression from an initial value of 1×10^6 s, with the ratio of successive time steps being 1.04. A Crank-Nicholson time scheme is used.

A series type analytical solution for the column effluent concentration as a function of time was given by Bastian and Lapidus (1956). For the parameter values used in this case, 20 terms of the series yield a converged solution.

As shown in Figure 12, the values calculated using MOTIF are very close to those calculated using the analytical solution.

2.6 CASE 6: SOLUTE TRANSPORT ALONG A DISCRETE FRACTURE WITH DIFFUSION INTO THE BACKGROUND ROCK MASS

This case simulates solute transport along a thin, water-filled fracture in a saturated background rock mass. Groundwater flows along the fracture with constant, uniform velocity, and a constant concentration radionuclide source exists at the origin of the fracture (Figure 13). The following assumptions are made:

(1) The width of the fracture is much smaller than its length.
(2) There is complete mixing across the fracture at all times.
(3) The permeability of the background rock mass is extremely low, such that only molecular diffusion occurs within it.
(4) Transport within the fracture is much faster than within the background rock mass.

The processes considered are advection along the fracture, hydrodynamic dispersion along the fracture, molecular diffusion within the background rock mass, linear equilibrium sorption onto the wall of the fracture, linear equilibrium sorption within the background rock mass and radioactive decay.

The solute concentration distribution in the background rock mass can be described by the equation:

$$D_d \frac{\partial^2 C}{\partial x^2} - \lambda C = \frac{\partial C}{\partial t} \qquad \textbf{(6.1)}$$

where: D_d = effective molecular diffusion coefficient.

The solute concentration distribution in the fracture can be described by the equation:

$$D \frac{\partial^2 C}{\partial z^2} - u \frac{\partial C}{\partial z} - \lambda C + \frac{\theta D_d}{\beta} \frac{\partial C}{\partial x}\Bigg|_{x=-\beta/2}^{x=\beta/2} = \frac{\partial C}{\partial t} \qquad \textbf{(6.2)}$$

where: θ = porosity.

The boundary conditions are:

$$C = C^* \qquad \text{at } x = 0,\ z = 0 \qquad \text{for } t > 0 \qquad \textbf{(6.3a)}$$

$$C = 0 \qquad \text{at } x = \infty \qquad \textbf{(6.3b)}$$

$$C = 0 \qquad \text{at } z = \infty. \qquad \textbf{(6.3c)}$$

Initially the concentrations are zero everywhere, i.e.:

$$C = 0 \qquad \text{at } t = 0. \tag{6.4}$$

The input parameter values are listed in Table 6.

In the MOTIF simulation the background rock mass is discretized using 1000 rectangular elements and the fracture is discretized using 25 line elements (Figure 14). The solution time steps increase in a geometric progression from an initial value of 8.64×10^6 s, with the ratio of successive time steps being 1.101. A Crank-Nicholson time scheme is used.

An analytical solution for the concentration distribution was given by Tang et al. (1981).

The comparison of the results calculated using the two methods is done in terms of concentration relative to the source concentration, i.e.: C/C*.

As shown in Figure 15, the agreement is very good, except at early time.

2.7 CASE 7: TWO DIMENSIONAL STEADY STATE GROUNDWATER FLOW AND SOLUTE TRANSPORT IN AN UNCONFINED AQUIFER

This case simulates the steady-state groundwater flow and transport of a conservative solute in a 250-m long, saturated, unconfined aquifer comprised of a fine, silty sand, within which a discontinuous, 2-m thick, medium-grained, sand layer is located (Figure 16).

Both geologic units are homogeneous and isotropic. The top boundary is a free-surface water table along which a recharge rate of 0.1 m/a is specified. The solute source is a prescribed concentration over a portion of the water table for a finite duration.

The hydraulic head distribution in the aquifer can be described by the equation:

$$\frac{\partial}{\partial x}\left(K\frac{\partial h}{\partial x}\right)+\frac{\partial}{\partial z}\left(K\frac{\partial h}{\partial z}\right)=0. \tag{7.1}$$

The solute concentration distribution in the aquifer can be described by the equation:

$$\frac{\partial}{\partial x}\left[D_{xx}\frac{\partial C}{\partial x}+D_{xz}\frac{\partial C}{\partial z}\right]+\frac{\partial}{\partial z}\left[D_{zz}\frac{\partial C}{\partial z}+D_{zx}\frac{\partial C}{\partial x}\right]-u_x\frac{\partial C}{\partial x}-u_z\frac{\partial C}{\partial z}=\frac{\partial C}{\partial t} \tag{7.2}$$

where: D_{xx}, D_{xz}, D_{zz} and D_{zx} are components of the hydrodynamic dispersion tensor
u_x = x component of the average linear velocity
u_z = z component of the average linear velocity.

The components of the hydrodynamic dispersion tensor are given by:

$$D_{xx} = a_L \frac{u_x^2}{|u|} + a_T \frac{u_z^2}{|u|} + D_d \qquad \textbf{(7.3a)}$$

$$D_{zz} = a_T \frac{u_x^2}{|u|} + a_L \frac{u_z^2}{|u|} + D_d \qquad \textbf{(7.3b)}$$

$$D_{xz} = D_{zx} = (a_L - a_T)\frac{u_x u_z}{|u|} \qquad \textbf{(7.3c)}$$

where: a_L = longitudinal dispersivity
a_T = transverse dispersivity.

The components of the average linear velocity are given by Darcy's law:

$$u_x = -\frac{K}{\theta}\frac{\partial h}{\partial x} \qquad \textbf{(7.4a)}$$

$$u_z = -\frac{K}{\theta}\frac{\partial h}{\partial z}. \qquad \textbf{(7.4b)}$$

For the top boundary the recharge rate is:

$$q_R^B = 3.17 \times 10^{-9} \text{ m/s } (=0.1 \text{ m/a}). \qquad \textbf{(7.5a)}$$

For the right hand boundary:

$$h = 5.375 \text{ m} \qquad \text{at } x = 250 \text{ m}. \qquad \textbf{(7.5b)}$$

The other boundaries are impermeable, i.e.:

$$\frac{\partial h}{\partial x} = 0 \qquad \text{at } x = 0 \qquad \textbf{(7.5c)}$$

$$\frac{\partial h}{\partial z} = 0 \qquad \text{at } z = 0. \qquad \textbf{(7.5d)}$$

The boundary conditions for solute transport on the top boundary (water table) are:

$$C = 1 \text{ ppm} \qquad \text{at } 40 \le x \le 80 \text{ m} \qquad \text{for } 0 < t \le 1.58 \times 10^8 \text{ s } (=5a) \qquad \textbf{(7.6a)}$$

$$C = 0 \qquad \text{at } 40 \le x \le 80 \text{ m} \qquad \text{for } t > 1.58 \times 10^8 \text{ s } (=5a) \qquad \textbf{(7.6b)}$$

$$C = 0 \qquad \text{at } x < 40 \text{ m}, x > 80 \text{ m} \qquad \text{for } t > 0. \qquad \textbf{(7.6c)}$$

The other boundary conditions for solute transport are:

$$C = 0 \qquad \text{at } x = 0 \qquad \textbf{(7.6d)}$$

$$\frac{\partial C}{\partial x} = 0 \qquad \text{at } x = 250 \text{ m} \qquad \textbf{(7.6e)}$$

$$\frac{\partial C}{\partial z} = 0 \qquad \text{at } z = 0. \qquad \textbf{(7.6f)}$$

Initially the concentrations are zero everywhere, i.e.:

$$C = 0 \qquad \text{at } t = 0. \qquad \textbf{(7.7)}$$

The input parameter values used are listed in Table 7.

In the MOTIF simulation the aquifer is divided into 2600 planar elements. The water table position is determined iteratively using a tolerance of 0.01% on the difference between the hydraulic head and the elevation of the water table nodes. A total of 5 iterations are required for convergence. During the iteration the positions of the top 10 layers of nodes are adjusted proportionately to minimize differences in sizes of adjacent elements. The mesh configuration at the end of the flow simulation (Figure 17) is used for the transport simulation. For the transport simulation a Crank-Nicholson time scheme and 92 time steps are used. The time steps increase in a geometric progression from an initial value of 100 s to a maximum value of 7.884×10^6 s, with the ratio of successive time steps being 2.5 until the maximum is reached.

The problem was initially solved by Sudicky (1989). The solution of the groundwater flow problem was obtained using the dual formulation model of Frind and Matanga (1985). The water table position was determined iteratively using a tolerance of 0.01% on the difference between the hydraulic head and the elevation of the water table nodes. The solution for solute transport was obtained using the Laplace transform Galerkin finite element technique.

In Figure 18, the concentration distributions at t = 8, 12, and 20 a, as calculated using the two methods, are compared. The agreement is good.

2.8 CASE 8: FULLY COUPLED FLUID FLOW AND HEAT TRANSPORT

This case simulates heat transport and density-driven fluid flow caused by a uniform spherical heat source with an exponentially decaying power output located in an infinite, saturated, permeable rock mass. This is the HYDROCOIN Level 1 Case 4. The rock mass is isotropic and homogeneous. The region of the heat source has the same properties as the surrounding rock.

Flow transients arising from compressibility effects are neglected. The density of fluid is assumed to vary linearly with temperature and to be independent of pressure. The viscosity of fluid is assumed to be independent of temperature and pressure. Thermal dispersion is assumed to be negligible.

The hydraulic head distribution in the rock mass can be described by the equation:

$$\frac{\rho_o g k}{\mu}\frac{\partial}{\partial x_i}\left[\rho\frac{\partial}{\partial x_i}\left(h+\frac{\Delta\rho}{\rho_o}x_3\right)\right]=-\theta\beta_w\rho_o\frac{\partial T}{\partial t} \qquad \textbf{(8.1)}$$

where:
- x_i = Cartesian coordinates, where subscript i varies from 1 to 3, and x_3 is vertical with upward being positive
- ρ_o = fluid reference density
- k = permeability
- $\Delta\rho$ = $\rho-\rho_o$ = difference between fluid density and fluid reference density
- β_w = fluid thermal expansion coefficient
- T = temperature.

Repeated subscripts denote summation in this and all following equations.

The temperature distribution in the rock mass can be described by the equation:

$$\lambda^T\frac{\partial}{\partial x_i}\left(\frac{\partial T}{\partial x_i}\right)-\theta c_f'\frac{\partial}{\partial x_i}(\rho u_i T)+\Phi_T=\frac{\partial}{\partial t}\left(\left[\theta\rho c_f'+(1-\theta)\rho_s c_s'\right]T\right) \qquad \textbf{(8.2)}$$

where:
- λ^T = effective thermal conductivity
- c_f' = fluid specific heat
- u_i = i-th component of average linear velocity
- Φ_T = heat source term
- ρ_s = density of the solid phase of the rock
- c_s' = specific heat of solid phase of the rock.

The components of the average linear velocity are given by Darcy's law:

$$u_i = -\frac{\rho_o g k}{\theta \mu} \frac{\partial}{\partial x_i}\left(h + \frac{\Delta\rho}{\rho_o} x_3\right) . \qquad \textbf{(8.3)}$$

The boundary conditions are:

$$h = 0 \qquad \text{at } W = \infty \qquad \textbf{(8.4a)}$$

$$T = 0 \qquad \text{at } W = \infty \qquad \textbf{(8.4b)}$$

where: $W = \left(x_1^2 + x_2^2 + x_3^2\right)^{1/2}$ is the spherical radial coordinate.

Initially the heads and temperatures are zero everywhere, i.e.:

$$h = 0 \qquad \text{at } t = 0 \qquad \textbf{(8.5a)}$$

$$T = 0 \qquad \text{at } t = 0. \qquad \textbf{(8.5b)}$$

The heat source term is:

$$\Phi_T = \frac{3Q_T}{4\pi r_s^3} \exp(-\lambda_t t) \cdot H(r_s - W) \qquad \text{for } t > 0 \qquad \textbf{(8.6)}$$

where: Q_T = initial power output from the heat source
r_s = radius of the spherical heat source
λ_t = decay constant for the heat source
H = Heaviside's unit function.

The relationship between fluid density and temperature is:

$$\rho = \rho_o(1 - \beta_w T) . \qquad \textbf{(8.7)}$$

The input parameter values used are listed in Table 8.

In the MOTIF simulation the flow domain extends to a distance twelve times the source radius, where increases in head and temperature are calculated to be negligible. Because of symmetry, only a segment of the spherical flow domain is discretized. A slice bounded by two vertical planes subtending a 15° angle is discretized using 832 3D solid elements (Figure 19).

The solution time stepping sequence is as follows: 40 steps of 0.5 a, 30 steps of 1.0 a, 25 steps of 2.0 a, 40 steps of 10.0 a, 40 steps of 12.5 a, 40 steps of 25 a, and 40 steps of 200 a. A fully implicit time scheme is used for the fluid flow equation and a Crank-Nicholson scheme for the heat transport equation. The fluid density is updated at each time step based on the temperature at the previous time, but no iteration is performed at a point in time.

An approximate analytical solution for the dynamic pressure rise distribution and temperature rise distribution was given by Hodgkinson (1980). The principal approximation was that variations in fluid density are included only in the buoyancy term, i.e. the Boussinesq approximation. The dynamic pressure rise (i.e. the actual pressure minus the hydrostatic pressure) is defined as:

$$p_d = \rho_o \, g \, h \ . \tag{8.8}$$

In Figure 20, the temperature rise at various times as a function of vertical distance above the centre of the heat source as calculated using the two methods are compared. A similar comparison for the dynamic pressure rise is shown in Figure 21. Excellent agreement has been achieved.

2.9 CASE 9: FULLY COUPLED FLUID FLOW AND SOLUTE TRANSPORT

This case simulates solute transport and density-driven fluid flow caused by constant solute sources and sinks in a vertical, two-dimensional square of saturated, homogeneous, isotropic porous media (Figure 22). Flow transients arising from compressibility effects are neglected. The density of fluid is assumed to vary linearly with solute concentration and to be independent of pressure. The viscosity of fluid is assumed to be independent of concentration. Mechanical dispersion is assumed to be negligible.

The hydraulic head distribution in the medium can be described by the equation:

$$\frac{\rho_o g k}{\mu} \frac{\partial}{\partial x_i}\left[\rho \frac{\partial}{\partial x_i}\left(h + \frac{\Delta\rho}{\rho_o} x_2\right)\right] = \theta \, \varepsilon \, \rho_o \frac{\partial C}{\partial t} \tag{9.1}$$

where: x_i = Cartesian coordinate where subscript i takes on values 1 and 2, and x_2 is vertical with upward being positive

ε = coefficient in fluid density equation.

The solute concentration distribution in the medium can be described by the equation:

$$D_d \frac{\partial}{\partial x_i}\left(\frac{\partial C}{\partial x_i}\right) - \frac{\partial}{\partial x_i}(u_i C) = \frac{\partial C}{\partial t} \ . \tag{9.2}$$

The components of the average linear velocity are given by Darcy's law:

$$u_i = -\frac{\rho_o g k}{\theta \mu} \frac{\partial}{\partial x_i}\left(h + \frac{\Delta\rho}{\rho_o} x_2\right) . \qquad \textbf{(9.3)}$$

The boundary conditions are:

$$q_F^B = 0 \qquad \text{at } x_1 = 0 \text{ and } x_1 = 20 \text{ m} \qquad \textbf{(9.4a)}$$

$$q_F^B = 0 \qquad \text{at } x_2 = 0 \text{ and } x_2 = 20 \text{ m} \qquad \textbf{(9.4b)}$$

$$C = 1 \qquad \text{at } 0 \le x_1 \le 10 \text{ m}, x_2 = 20 \text{ m} \qquad \text{for } t > 0 \text{ s} \qquad \textbf{(9.4c)}$$

$$C = 0 \qquad \text{at } 10 < x_1 \le 20 \text{ m}, x_2 = 20 \text{ m} \qquad \textbf{(9.4d)}$$

$$C = 0 \qquad \text{at } x_2 = 0 \qquad \textbf{(9.4e)}$$

$$\frac{\partial C}{\partial x_1} = 0 \qquad \text{at } x_2 = 0 \text{ and } x_2 = 20 \text{ m} \qquad \textbf{(9.4f)}$$

where: q_F^B = fluid mass flux normal to the boundary.

Initially the heads and concentrations are zero everywhere, i.e.:

$$h = 0 \qquad \text{at } t = 0 \qquad \textbf{(9.5a)}$$

$$C = 0 \qquad \text{at } t = 0. \qquad \textbf{(9.5b)}$$

The relationship between fluid density and solute concentration is:

$$\rho = \rho_o(1 + \varepsilon C) . \qquad \textbf{(9.6)}$$

The input parameter values used are listed in Table 9.

In the MOTIF simulation the medium is divided into 400 uniform, square, planar elements. Uniform solution time steps of 26572 s are used. A fully implicit time scheme is used for the fluid flow equation and a Crank-Nicholson scheme for the solute transport equation. At each time step Picard iteration is performed until the solution converges. The convergence tolerance is 10 m for head and 0.1 for concentration. A maximum of 4 iterations are performed.

An approximate solution was calculated by Diersch (1981), also using the finite element method. This solution included the Boussinesq approximation.

The comparison of the results calculated using the MOTIF code and Diersch's solution is done in terms of the concentration distribution at various dimensionless times. Dimensionless time is defined by:

$$t^+ = \frac{D_d t}{x_L} \quad . \tag{9.7}$$

In Figure 23, concentration contours at a dimensionless time of 0.01 as calculated by the two simulations are shown. Errors associated with transferring the contours from Diersch's paper are likely of similar magnitude to the actual differences between the results of the simulations.

2.10 CASE 10: RISE OF A GROUNDWATER MOUND DUE TO INFILTRATION FROM A STRIP RECHARGE PIT

This case simulates the rise of the free-surface water table beneath and in the vicinity of an artificial recharge pit overlying a saturated, unconfined, horizontal aquifer having an impermeable base. The recharge pit is of infinite length, finite width and is located midway between two constant head boundaries. Because of symmetry, only one half of the system need be modelled (Figure 24). It is assumed that the aquifer is homogeneous, isotropic and incompressible, and the fluid is incompressible. Initially the water table is horizontal. The recharge rate is uniform and constant.

Assuming that the rise in the water table is small compared to the initial thickness of the zone of saturation, i.e. the Dupuit approximation, the water table can be described by the equation:

$$K b_{ao} \frac{\partial^2 h}{\partial x^2} + \Phi_F = \theta \frac{\partial h}{\partial t} \tag{10.1}$$

where: b_{ao} = initial thickness of the zone of saturation.

For the left hand (upstream) boundary:

$$\frac{\partial h}{\partial x} = 0 \qquad \text{at } x = 0 \text{ m.} \tag{10.2a}$$

For the right hand boundary:

$$h = 0 \text{ m} \qquad \text{at } x = 85 \text{ m.} \tag{10.2b}$$

Initially the heads are zero everywhere, i.e.:

$$h = 0 \qquad \text{at } t = 0. \tag{10.3}$$

The fluid source term is:

$$\Phi_F = q_R^B \qquad \text{at } 0 \le x \le 5 \text{ m} \qquad \text{for } t > 0 \tag{10.4a}$$

$$\Phi_F = 0 \qquad \text{at } 5 < x \le 85 \text{ m.} \tag{10.4b}$$

The input parameter values used are listed in Table 10.

In the MOTIF simulation the domain is discretized into 85 uniform line elements having cross sectional areas of 6.1 m. The solution time steps increase in a geometric progression from an initial value of 100 s to a maximum value of 1000 s with the ratio of successive time steps being 1.2. A fully implicit time scheme is used.

An analytical solution for the rise of the water table was given by Amar (1975).

The comparison of the results calculated using the two methods is done in terms of dimensionless water table rise versus dimensionless time at various dimensionless distances.

Dimensionless distance is defined by:

$$x^+ = \frac{x}{x_L} \,. \tag{10.5}$$

Dimensionless time is defined by:

$$t^+ = \frac{K b_{a_o} t}{\theta x_R^2} \tag{10.6}$$

where: x_R = half width of recharge pit.

Dimensionless water table rise is defined by:

$$h^+ = \frac{K b_{a_o} h}{q_R^B x_R^2} \,. \tag{10.7}$$

As shown in Figure 25, for the values calculated at dimensionless distances of 0.1 and 5.1 the agreement is very good.

2.11 CASE 11: DRAINAGE OF WATER FROM A SAND COLUMN

This case simulates the gravity driven drainage of water from a one-dimensional column of homogeneous sand which is initially saturated (Figure 26). Both the water and sand are considered to be incompressible. The pressure at the bottom of the column is maintained at atmospheric value. Initially the pressure head distribution varies linearly from the air entry value of -0.4 m at the top of the column to zero at the bottom.

The hydraulic head distribution in the column can be described by the equation:

$$\frac{k}{\mu}\frac{\partial}{\partial z}\left(k^r\frac{\partial h}{\partial z}\right)=\theta\frac{\partial S_u}{\partial p}\frac{\partial h}{\partial t} \qquad \textbf{(11.1)}$$

where: k^r = relative permeability
S_u = degree of saturation
p = fluid pressure.

The boundary conditions are:

$$h = 0 \qquad \text{at } z = 0 \qquad \textbf{(11.2a)}$$

$$\frac{\partial h}{\partial z}=0 \qquad \text{at } z = 0.57 \text{ m.} \qquad \textbf{(11.2b)}$$

The initial conditions are:

$$h = 0.298\, z \qquad \text{at } t = 0. \qquad \textbf{(11.3)}$$

The characteristic curves for the drainage of water from the sand are shown in Figure 27. The other input parameters used are listed in Table 11.

In the MOTIF simulation the column is divided into 20 uniform solid elements with dimensions 2.5 cm x 2.5 cm x 2.9 cm. Equal time steps of 4 s are used. At each time step only one iteration is required for convergence of the solution to within a tolerance of 0.01 m. A fully implicit time scheme is used.

A solution was previously calculated by Whisler and Watson (1968) using the finite difference method.

The comparison of the results of the two different simulations is done in terms of the pressure head:

$$\psi = h - z\,. \qquad \textbf{(11.4)}$$

Figure 26 shows the calculated pressure head versus time at two locations in the column. The agreement between the two solutions is good.

2.12 CASE 12: STEADY-STATE DIPOLAR GROUNDWATER FLOW IN A CONFINED AQUIFER

This case models the steady-state, two-dimensional flow in a saturated, infinite, confined, horizontal aquifer in which an injection and a withdrawal well 55 m apart are pumped at the same rate. The aquifer is homogeneous and isotropic.

The hydraulic head distribution in the aquifer can be described by the equation:

$$T_b\left(\frac{\partial^2 h}{\partial x^2}+\frac{\partial^2 h}{\partial y^2}\right)+\Phi_F=0\ . \qquad \textbf{(12.1)}$$

The boundary conditions are:

$$h = 0 \qquad \text{at } x = \pm\infty \qquad \textbf{(12.2a)}$$

$$h = 0 \qquad \text{at } y = \pm\infty. \qquad \textbf{(12.2b)}$$

Initially the heads are zero everywhere, i.e.:

$$h = 0 \qquad \text{at } t = 0. \qquad \textbf{(12.3)}$$

The fluid source term is:

$$\Phi_F = Q \qquad \text{at } x = -192.0 \text{ m}, y = 7.6 \text{ m} \qquad \text{for } t > 0 \qquad \textbf{(12.4a)}$$

$$\Phi_F = -Q \qquad \text{at } x = -197.7 \text{ m}, y = 62.3 \text{ m} \qquad \text{for } t > 0 \qquad \textbf{(12.4b)}$$

$$\Phi_F = 0 \qquad \text{at } (x,y) \neq (-192.0, 7.6) \text{ m or } (-197.7, 62.3) \text{ m}. \qquad \textbf{(12.4c)}$$

The input parameter values used are listed in Table 12.

In the MOTIF simulation a region measuring 2549 m x 2336 m is discretized using 3395 planar elements (Figure 28). The boundaries are at a sufficient distance from the wells so as not to influence the head changes caused by the pumping. The boundaries are assigned a head value of 0. The element size increases in a geometric progression with distance from the wells until a maximum size is reached. The smallest element is about 0.25 m, the largest is 40 m, and the ratio of adjacent elements is about 1.4:1 or less.

An analytical solution for the hydraulic head distribution was given by Bear (1972).

Figure 29 shows the hydraulic head distribution along the line passing through the injection and withdrawal well as calculated using the two methods. The agreement is very good.

2.13 CASE 13: SOLUTE TRANSPORT IN A DIPOLAR GROUNDWATER FLOW FIELD IN A CONFINED AQUIFER

This case models the advection and longitudinal dispersion of a conservative solute in the steady-state, two-dimensional, dipolar flow field of Case 12. The solute is introduced over an 8 hour period at the injection well.

The solute concentration distribution in the aquifer can be described by the equation:

$$\frac{\partial}{\partial x}\left[D_{xx}\frac{\partial C}{\partial x}+D_{xy}\frac{\partial C}{\partial y}\right]+\frac{\partial}{\partial y}\left[D_{yy}\frac{\partial C}{\partial y}+D_{yx}\frac{\partial C}{\partial x}\right]-u_x\frac{\partial C}{\partial x}-u_y\frac{\partial C}{\partial y}+\Phi_c=\frac{\partial C}{\partial t} \qquad \textbf{(13.1)}$$

where: D_{xx}, D_{xy}, D_{yy} and D_{yx} are components of the hydrodynamic dispersion tensor
u_y = y component of the average linear velocity
Φ_c = solute source term.

The components of the hydrodynamic dispersion tensor are given by:

$$D_{xx}=a_L\frac{u_x^2}{|u|} \qquad \textbf{(13.2a)}$$

$$D_{yy}=a_L\frac{u_y^2}{|u|} \qquad \textbf{(13.2b)}$$

$$D_{xy}=D_{yx}=a_L\frac{u_x u_y}{|u|}\ . \qquad \textbf{(13.2c)}$$

The components of the average linear velocity are given by Darcy's law:

$$u_x=-\frac{T_b}{b_a\theta}\frac{\partial h}{\partial x} \qquad \textbf{(13.3a)}$$

$$u_y=-\frac{T_b}{b_a\theta}\frac{\partial h}{\partial y}\ . \qquad \textbf{(13.3b)}$$

At the withdrawal well the boundary condition is:

$$\frac{\partial C}{\partial x} = \frac{\partial C}{\partial y} = 0 \qquad \text{at } x = -197.7 \text{ m}, y = 62.3 \text{ m}. \qquad \textbf{(13.4a)}$$

The other boundary conditions are:

$$\frac{\partial C}{\partial x} = 0 \qquad \text{at } x = \pm \infty \qquad \textbf{(13.4b)}$$

$$\frac{\partial C}{\partial y} = 0 \qquad \text{at } y = \pm \infty. \qquad \textbf{(13.4c)}$$

Initially the concentrations are zero everywhere, i.e.:

$$C = 0 \qquad \text{at } t = 0. \qquad \textbf{(13.5)}$$

The solute source term is:

$$\Phi_c = 5 \times 10^{-4} \text{ kg/s} \qquad \text{at } x = -192.0, y = 7.6 \text{ m} \qquad \text{for } 0 < t \leq 2.88 \times 10^4 \text{ s } (= 8 \text{ hrs}) \qquad \textbf{(13.6a)}$$

$$\Phi_c = 0 \qquad \text{at } x = -192.0, y = 7.6 \text{ m} \qquad \text{for } t > 2.88 \times 10^4 \text{ s} \qquad \textbf{(13.6b)}$$

$$\Phi_c = 0 \qquad \text{at } (x,y) \neq (-192.0, 7.6) \text{ m} \qquad \text{for } t > 0. \qquad \textbf{(13.6c)}$$

The input parameter values used are listed in Table 13.

The MOTIF simulation uses the same finite element mesh that was used in Case 12 (Figure 28). The perimeter of the mesh has a prescribed dispersive flux of value 0. A fully implicit time scheme and 315 time steps are used in the solution. The size of time step increases in a geometric progression from an initial value of 0.25 s until the end of the 8-hour solute injection period. The ratio of successive time steps is 1.091. To ensure accurate representation of the sudden change in injection concentration, the original initial value is used for the next time step, and subsequent steps increase in the same geometric progression as before until a maximum value of 8640 s is reached.

An approximate analytical solution for the solute concentration that appears at the withdrawal well as a function of time was given by Gelhar (1982). This solution assumes that the solute was introduced instantaneously at the injection well.

As shown in Figure 30, the values calculated using MOTIF are very close to those calculated using the analytical solution. The slightly greater dispersion of the MOTIF curve is expected because of the non-instantaneous injection of the solute.

2.14 THE HENRY PROBLEM - FULLY COUPLED FLUID FLOW AND SOLUTE TRANSPORT

This case simulates solute transport and density-driven fluid flow in a saturated, homogeneous, isotropic, semi-infinite aquifer that is bounded above and below by an impermeable boundary, is recharged on one side by a constant freshwater influx, and is exposed on the other side to a stationary body of seawater (Figure 31). This problem was originally posed by Henry (1964). Flow transients arising from compressibility effects are neglected. The density of fluid is assumed to vary linearly with solute concentration and to be independent of pressure. The viscosity of the fluid is assumed to be independent of concentration. Mechanical dispersion is assumed to be negligible. The value of the effective molecular diffusion coefficient and the boundary condition on the seaward side are the same as those used by Frind (1982).

The hydraulic head distribution in the aquifer can be described by Equation (9.1).

The solute concentration distribution in the aquifer can be described by Equation (9.2).

The components of the average linear velocity are given by Darcy's law, Equation (9.3).

The boundary conditions are:

$$h = \frac{\rho_B}{\rho_o}(1 - x_2) + x_2 \qquad \text{at } x_1 = 2 \text{ m} \qquad \text{for } t > 0 \qquad \textbf{(14.1a)}$$

$$q_F^B = 0.066\,\text{kg}/\text{s}\cdot\text{m}^2 \qquad \text{at } x_1 = 0 \qquad \text{for } t > 0 \qquad \textbf{(14.1b)}$$

$$q_F^B = 0 \qquad \text{at } x_2 = 0 \text{ and } x_2 = 1 \text{ m} \qquad \textbf{(14.1c)}$$

$$C = 0 \qquad \text{at } x_1 = 0 \qquad \textbf{(14.1d)}$$

$$C = 1 \qquad \text{at } x_1 = 2 \text{ m}, 0 \le x_2 < 0.8 \text{ m} \qquad \text{for } t > 0 \qquad \textbf{(14.1e)}$$

$$\frac{\partial C}{\partial x_1} = 0 \qquad \text{at } x_1 = 2 \text{ m}, 0.8 \le x_2 \le 1 \text{ m} \qquad \textbf{(14.1f)}$$

$$\frac{\partial C}{\partial x_2} = 0 \qquad \text{at } x_2 = 0 \text{ and } x_2 = 1 \text{ m} \qquad \textbf{(14.1g)}$$

where: ρ_B = seawater density.

Initially the heads and concentrations are uniform and have the following values:

$$h = 1 \qquad \text{at } t = 0 \tag{14.2a}$$

$$C = 0 \qquad \text{at } t = 0. \tag{14.2b}$$

The relationship between fluid density and solute concentration is described by Equation 9.6.

The input parameter values are listed in Table 14.

In the MOTIF simulation the medium is divided into 200 uniform, square, planar elements. The system is simulated up to a time of 21 600 s (360 min.), by which time equilibrium conditions are attained. The solution time steps increase in a geometric progression from an initial value of 12 s to a maximum value of 600 s, with the ratio of successive time steps being 1.11 until the maximum is reached. A fully implicit time scheme is used for the fluid flow equation and a Crank-Nicholson scheme for the solute transport equation. The fluid density is updated at each time step based on the concentration at the previous time, but no iteration is performed at a point in time.

Figure 32 shows the equilibrium solute concentration contours in the aquifer as calculated using MOTIF, and as calculated by Frind (1982), who also used the finite element method. The agreement between the two solutions is good.

3. CONCLUSIONS

It is evident from the graphical comparisons presented that the MOTIF solutions for the fourteen verification cases are generally in excellent agreement with known analytical or numerical solutions obtained from independent sources.

This series of verification studies has established the ability of the MOTIF finite-element code to accurately model the groundwater flow and solute and heat transport phenomena for which it is intended.

ACKNOWLEDGEMENTS

J. Halley provided assistance in preparing the final diagrams for this document. Word processing was ably performed by Heather Worona, Pat McCooeye and Wanda Farrell-Jansson. This work is funded jointly by AECL and Ontario Hydro under the auspices of the CANDU Owners Group.

REFERENCES

Amar, A.C. 1975. Theory of groundwater recharge for a strip basin. Groundwater, 13(3), 282-292.

Bastian, W.C. and L. Lapidus. 1956. Longitudinal diffusion in ion exchange and chromatographic columns: Finite column. J. Phys. Chem., 60, 816-817.

Bear, J. 1972. Dynamics of Fluids in Porous Media, American Elsevier, New York.

Chan, T., J.A.K. Reid and V. Guvanasen. 1987. Numerical modelling of coupled fluid, heat, and solute transport in deformable fractured rock. In Coupled Processes Associated with Nuclear Waste Repositories, Chin-Fu Tsang (Editor), Academic Press, Inc., Orlando, Florida, 605-625.

Diersch, H.J. 1981. Primitive variable finite element solutions of free convection flows in porous media. Zeitschrift Fuer Angewandte Mathematik Und Mechanik, 61(7), 325-337.

Frind, E.O. 1982. Simulation of long-term transient density-dependent transport in groundwater. Adv. Water Resour., 5, 73-78.

Frind, E.O. and G.B. Matanga. 1985. The dual formulation of flow for contaminant transport modeling, 1, Review of theory and accuracy aspects, Water Resour. Res., 21(2), 159-169.

Gelhar, L.W. 1982. Analysis of two-well tracer tests with a pulse input. Rockwell International, Rockwell Hanford Operations, RHO-BW-CR-131 P, Richland, WA.

Gringarten, A.C., H.J. Ramey and R. Raghaven. 1974. Unsteady-state pressure distributions created by a well with a single infinite-conductivity vertical fracture. Society of Petroleum Engineers Journal, 14(4), 347-360.

Grundfelt, B. 1984. Proposal for a test problem for HYDROCOIN Level 1, Case 2: Steady state flow in a rock mass intersected by permeable fracture zones, KEMAKTA Consultants Co., Stockholm, Sweden.

Guvanasen, V. 1985. Development of a finite-element code and its application to geoscience research. In Proc. 17th Information Meeting of the Nuclear Fuel Waste Management Program. Atomic Energy of Canada Limited Technical Record, TR-299.

Guvanasen, V. and T. Chan. In preparation. A finite element three-dimensional model of flow and transport in fractured/porous media (MOTIF): Mathematical formulation and user's manual. Atomic Energy of Canada Limited Report.

Henry, H.R. 1964. Effects of dispersion on salt encroachment in coastal aquifers. U.S.G.S. Water Supply Pap., 1613-C, C71-C84.

Hodgkinson, D. 1980. A mathematical model for hydrothermal convection around a radioactive waste depository in hard rock. Annals of Nuclear Energy, 7, 313-334.

Hodgkinson, D. and J. Barker. 1985. Specification of a test problem for HYDROCOIN Level 1, case 1: Transient flow from a borehole in a fractured permeable medium, U.K. Atomic Energy Authority, AERE-R11574, Harwell, U.K.

Marino, M.A. 1974. Distribution of contaminants in porous media flow. Water Resour. Res., 10(5), 1013-1018.

Sudicky, E.A. 1989. The Laplace transform Galerkin technique: a time-continuous finite element theory and application to mass transport in groundwater. Water Resour. Res., 25(8), 1833-1846.

Swedish Nuclear Power Inspectorate. 1988. The International HYDROCOIN Project - Level 1: Code Verification. OECD, Paris, France.

Tang, D.G., E.O. Frind and E.A. Sudicky. 1981. Contaminant transport in fractured porous media: analytical solution for a single fracture. Water Resour. Res., 17, 555.

Whisler, F.D. and K.K. Watson. 1968. One-dimensional gravity drainage of uniform columns of porous materials. Journal of Hydrology, 6, 277-296.

(TR- indicates unrestricted, unpublished reports available from SDDO, AECL, Chalk River Laboratories, Chalk River, Ontario K0J 1J0.)

NOMENCLATURE

SYMBOL	DEFINITION	UNIT
a_L	longitudinal dispersivity	m
a_T	transverse dispersivity	m
b_a	aquifer thickness	m
b_{ao}	initial thickness of the zone of saturation	m
C	solute concentration	ppm
C*	solute source concentration	ppm
c_f	fluid compressibility	Pa^{-1}
c_f'	fluid specific heat	J/kg·°C
c_s'	specific heat of the solid phase of the rock	J/kg·°C
D	hydrodynamic dispersion coefficient	m^2/s
D_d	effective molecular diffusion coefficient	m^2/s
D_{xx}, D_{xz}, D_{zz}, D_{zx}, D_{yy}, D_{xy}, D_{yx}	components of the hydrodynamic dispersion tensor	m^2/s
g	gravitational acceleration	m/s^2
H	Heaviside's unit function	-
h	hydraulic head	m
h_a	time dependent head in the borehole	m
h_o	initial head in the system	m
h_∞	asymptotic value of head in the borehole	m
h^+	dimensionless water table rise	-
K	hydraulic conductivity	m/s
K_b	hydraulic conductivity of the background rock mass	m/s
k	permeability	m^2
k^r	relative permeability	-
p	fluid pressure	Pa
p_d	dynamic pressure rise	Pa

Q	well pumping rate	m^3/s
Q_T	initial power output from the heat source	W
q_F^B	fluid mass flux normal to the boundary	$kg/s \cdot m^2$
q_R^B	recharge rate	m/s or m/a
q_T^B	energy conductive and dispersive flux normal to the boundary	W/m^2
R	retardation factor	-
r_s	radius of the spherical heat source	m
S_b	aquifer storativity	-
S_f	fracture storativity	-
S_s	specific storage of the background rock mass	m^{-1}
S_u	degree of saturation	-
T	temperature	°C
T_b	aquifer transmissivity	m^2/s
T_f	fracture transmissivity	m^2/s
t	time	s or a
t^+	dimensionless time	-
u	average linear velocity	m/s
u_i	i^{th} component of the average linear velocity	m/s
u_x, u_y, u_z	components of the average linear velocity	m/s
W	spherical radial coordinate	m
x, y, z	Cartesian coordinates	m
x_i, x_j	Cartesian coordinates	m
x_L	model length	m
x_r	half width of recharge pit	m
x_1, x_2, x_3	Cartesian coordinates	m
x^+	dimensionless distance	-
β	fracture aperture	m
β_w	fluid thermal expansion coefficient	$°C^{-1}$
Δh^+	dimensionless drawdown	-

$\Delta\rho$	difference between fluid density and fluid reference density	kg/m^3
ε	coefficient in fluid density equation	-
Φ_c	solute source term	kg/s
Φ_F	fluid source term	m/s
Φ_T	heat source term	W/m^3
Γ	boundary	-
λ	radioactive decay constant	s^{-1}
λ_T	decay constant for the heat source	s^{-1}
λ^T	effective thermal conductivity	W/m·°C
μ	fluid dynamic viscosity	Pa·s
θ	porosity	-
ρ	fluid density	kg/m^3
ρ_B	seawater density	kg/m^3
ρ_s	density of the solid phase of the rock	kg/m^3
ρ_o	fluid reference density	kg/m^3
ω	radial coordinate	m
ψ	pressure head	m

TABLE 1

CASE 1: INPUT PARAMETER VALUES

Parameter	Value
Hydraulic conductivity of background rock mass, K	1×10^{-8} m/s
Hydraulic conductivity of fracture zones, K	1×10^{-6} m/s

TABLE 2

CASE 2: INPUT PARAMETER VALUES

Parameter	Value
Aquifer thickness, b_a	1.0 m
Fracture aperture, β	0.01 m
Aquifer transmissivity, T_b	5×10^{-4} m^2/s
Aquifer storativity, S_b	0.001
Fluid density, ρ	1000 kg/m^3
Fluid dynamic viscosity, μ	0.001472 Pa·s
Fluid Compressibility, c_f	4.5×10^{-10} Pa^{-1}
Well pumping rate, Q	0.004 m^3/s

TABLE 3

CASE 3: INPUT PARAMETER VALUES

Parameter	Value
Hydraulic conductivity of background rock mass, K_b	1×10^{-9} m/s
Fracture transmissivity, T_f	1×10^{-8} m^2/s
Specific storage of background rock mass, S_s	1×10^{-7} m^{-1}
Fracture storativity, S_f	1×10^{-10}

TABLE 4

CASE 4: INPUT PARAMETER VALUES

Parameter	Value		
	Case a	Case b	Case c
Average linear velocity, u	0.001 m/s	0.001 m/s	0.001 m/s
Hydrodynamic dispersion coefficient, D	0.001 m^2/s	0.001 m^2/s	0.001 m^2/s
Radioactive decay constant, λ	0	0	3.633×10^{-5} s^{-1}
Retardation factor, R	0	1.8747	0

TABLE 5

CASE 5: INPUT PARAMETER VALUES

Parameter	Value
Average linear velocity, u	5×10^{-8} m/s
Hydrodynamic dispersion coefficient, D	2.5×10^{-6} m^2/s
Source solute concentration, C*	100 ppm

TABLE 6

CASE 6: INPUT PARAMETER VALUES

Parameter	Value
Fracture aperture, β	1×10^{-4} m
Porosity of background rock mass, θ	0.01
Average linear velocity along fracture, u	1.16×10^{-7} m/s
Hydrodynamic dispersion coefficient of fracture, D	5.99×10^{-8} m^2/s
Effective molecular diffusion coefficient of background rock mass, D	1.6×10^{-10} m^2/s
Radioactive decay constant, λ	1.78×10^{-9} s^{-1}

TABLE 7

CASE 7: INPUT PARAMETER VALUES

Parameter	Value
Hydraulic conductivity of fine silty sand, K	5×10^{-6} m/s
Hydraulic conductivity of medium-grained sand, K	1×10^{-4} m/s
Porosity, θ	0.35
Longitudinal dispersivity, a_L	0.5 m
Transverse dispersivity, a_T	0.005 m
Effective molecular diffusion coefficient, D_d	1.34×10^{-9} m^2/s

TABLE 8

CASE 8: INPUT PARAMETER VALUES

Parameter	Value
Radius of spherical heat source, r_s	250 m
Permeability, k	1×10^{-16} m^2
Porosity, θ	1×10^{-4}
Density of the solid phase of the rock, ρ_s	2600 kg/m^3
Specific heat of the solid phase of the rock, c_s'	879 J/kg·°C
Effective thermal conductivity, λ^T	2.51 W/m·°C
Fluid reference density, ρ_o	992.2 kg/m^3
Fluid dynamic viscosity, μ	6.529×10^{-4} Pa·s
Fluid thermal expansion coefficient, β_w	3.85×10^{-4} $°C^{-1}$
Fluid specific heat, c_f'	4200 J/kg·°C
Initial power output for heat source, Q_T	1×10^7 W
Decay constant for heat source, λ_T	7.3215×10^{-10} s^{-1}

TABLE 9

CASE 9: INPUT PARAMETER VALUES

Parameter	Value
Permeability, k	4.07×10^{-10} m^2
Porosity, θ	1.0
Fluid reference density, ρ_o	1000 kg/m^3
Fluid dynamic viscosity, μ	0.0013 Pa·s
Coefficient in fluid density equation, ε	0.025
Effective molecular diffusion coefficient, D_d	3.725×10^{-6} m^2/s

TABLE 10

CASE 10: INPUT PARAMETER VALUES

Parameter	Value
Hydraulic conductivity, K	9.423×10^{-4} m/s
Porosity, θ	0.35
Recharge rate, q_R^B	1×10^{-4} m/s

TABLE 11

CASE 11: INPUT PARAMETER VALUES

Parameter	Value
Permeability, k	2.626×10^{-11} m^2
Porosity, θ	0.35

TABLE 12

CASE 12: INPUT PARAMETER VALUES

Parameter	Value
Transmissivity, T_b	2.67×10^{-4} m^2/s
Well pumping rate, Q	3.334×10^{-4} m^3/s

TABLE 13

CASE 13: INPUT PARAMETER VALUES

Parameter	Value
Aquifer thickness, b_a	1.0 m
Porosity, θ	0.01
Longitudinal dispersivity, a_L	2.75 m

TABLE 14

CASE 14: INPUT PARAMETER VALUES

Parameter	Value
Permeability, k	1.02×10^{-9} m^2
Porosity, θ	0.35
Fluid reference density, ρ_o	1000 kg/m^3
Seawater density, ρ_B	1025 kg/m^3
Fluid dynamic viscosity, μ	0.001 Pa·s
Coefficient in fluid density equation, ε	0.025
Effective molecular diffusion coefficient, D_d	6.6×10^{-6} m^2/s

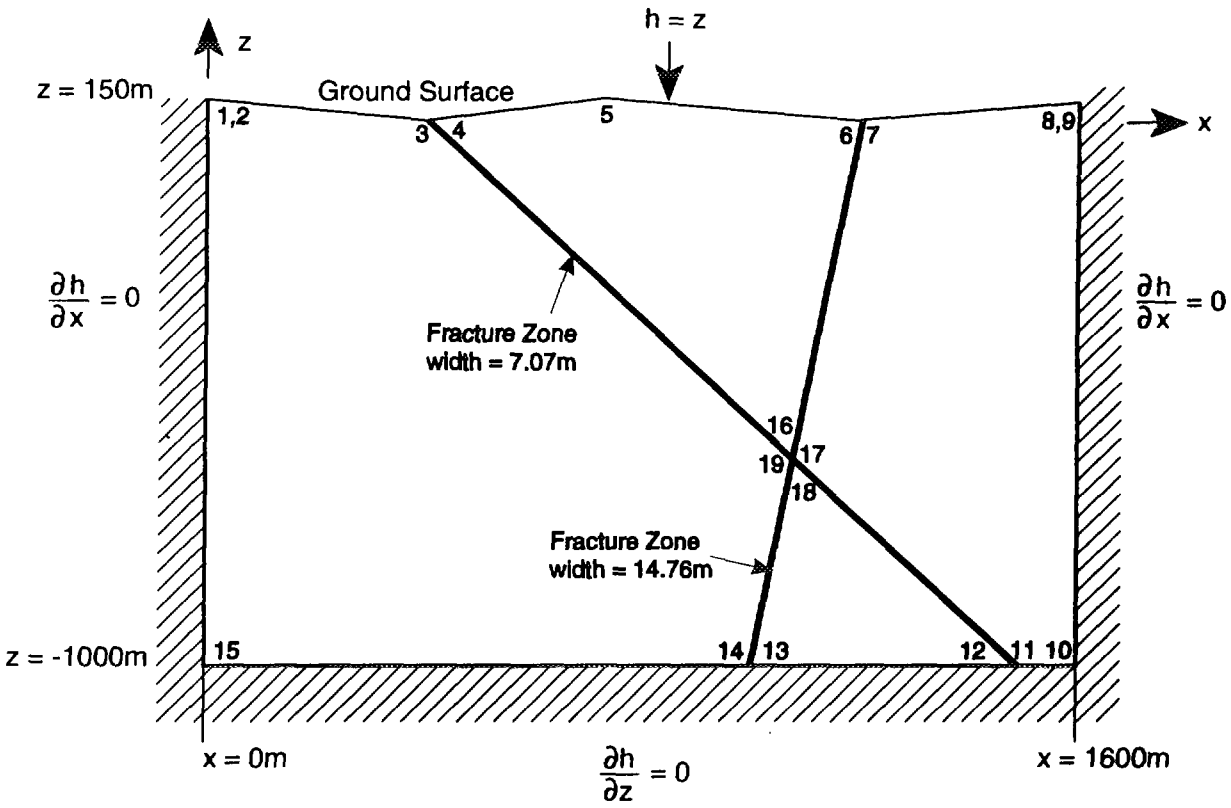

Point	Cartesian coordinates of point	
	x (m)	z (m)
1	0.	150.
2	10.	150.
3	395.	100.
4	405.	100.
5	800.	150.
6	1192.5	100.
7	1207.5	100.
8	1590.	150.
9	1600.	150.
10	1600.	-1000.
11	1505.	-1000.
12	1495.	-1000.
13	1007.5	-1000.
14	992.5	-1000.
15	0.	-1000.
16	1071.3462	-566.3459
17	1084.0385	-579.0383
18	1082.5	-587.5
19	1069.8077	-574.8077

FIGURE 1: Case 1: Model Geometry and Boundary Conditions

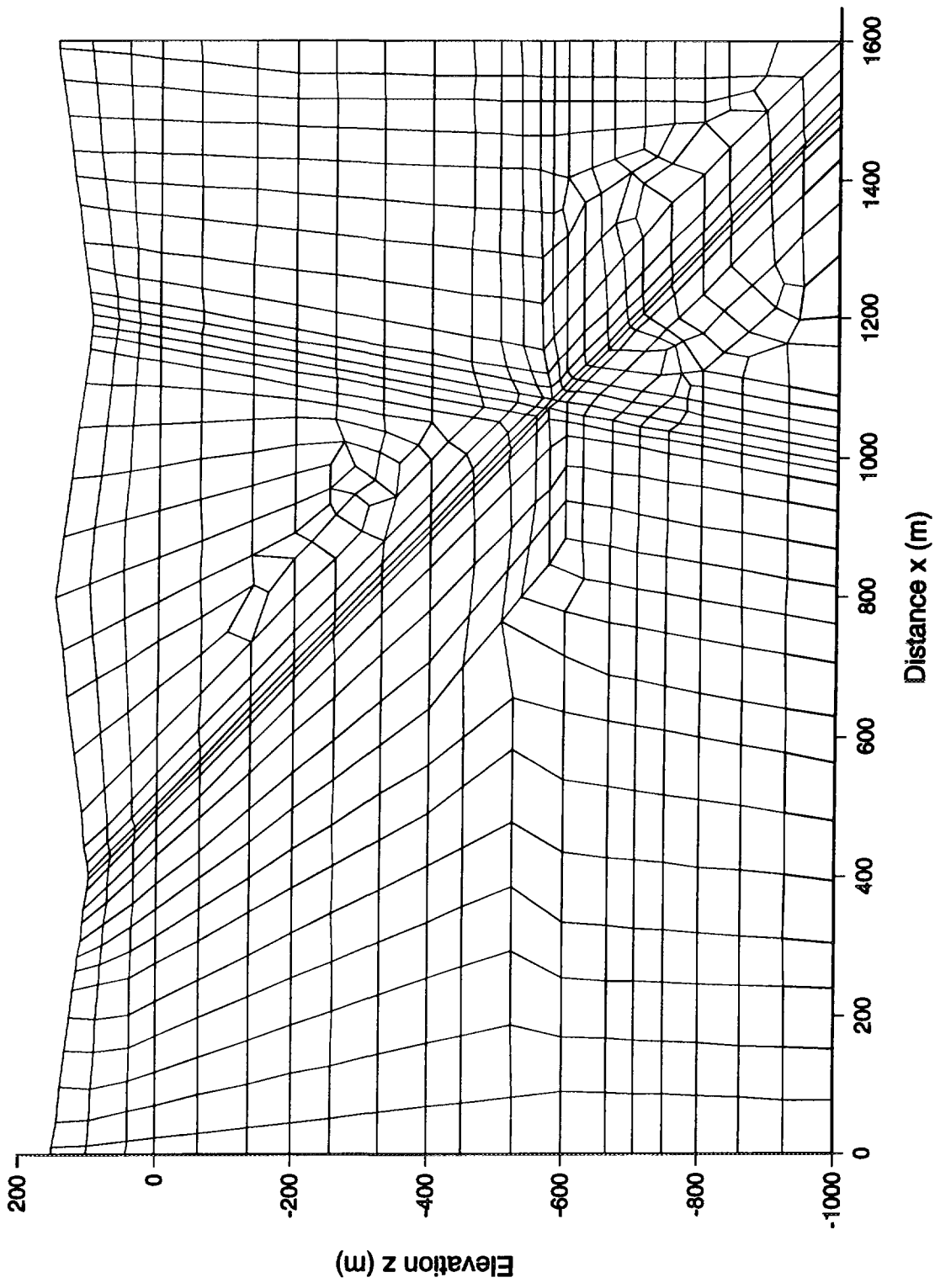

FIGURE 2: Case 1: MOTIF Spatial Discretization - Fine Mesh

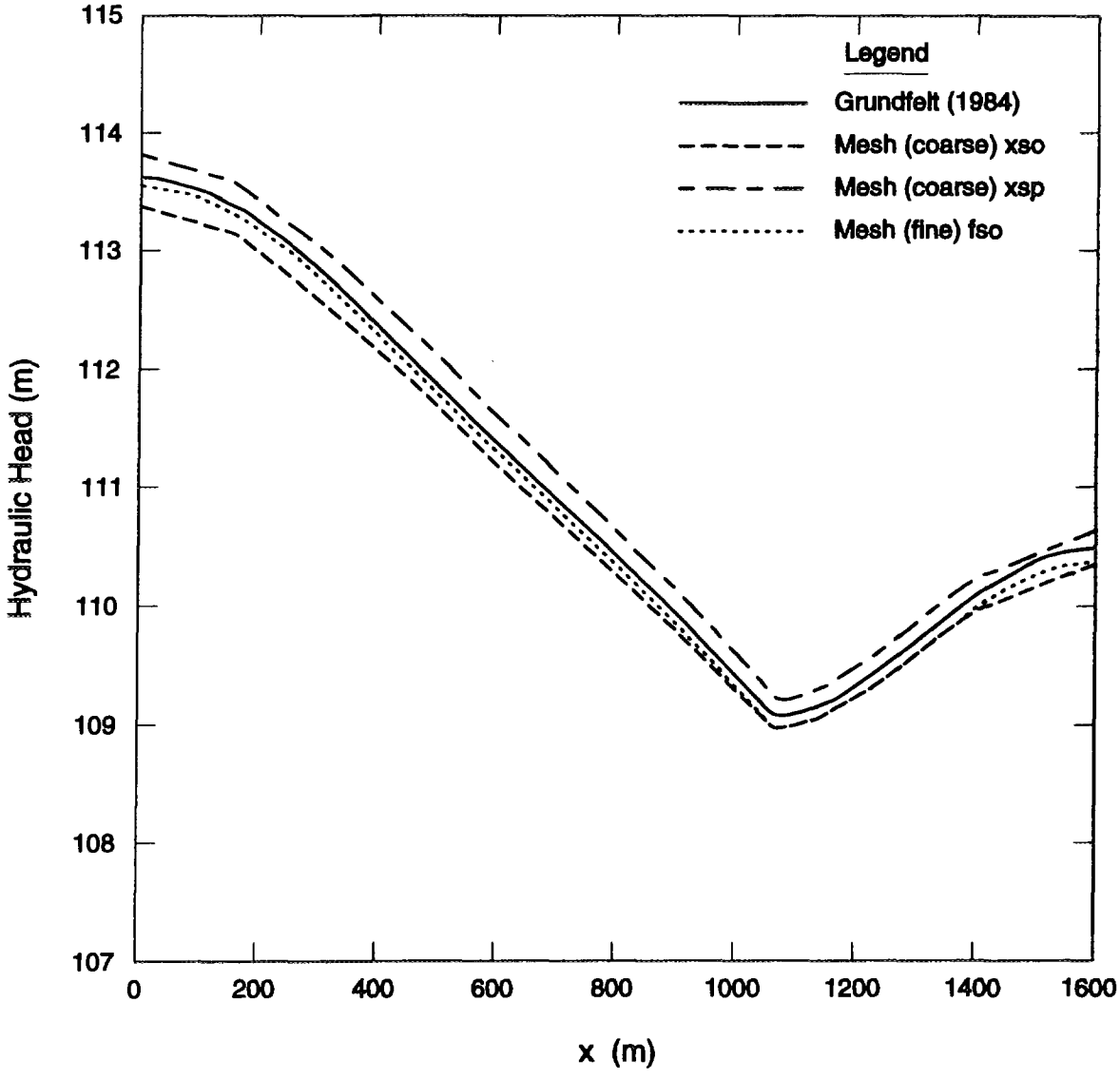

FIGURE 3: Case 1: Hydraulic Head at an Elevation z = -600m

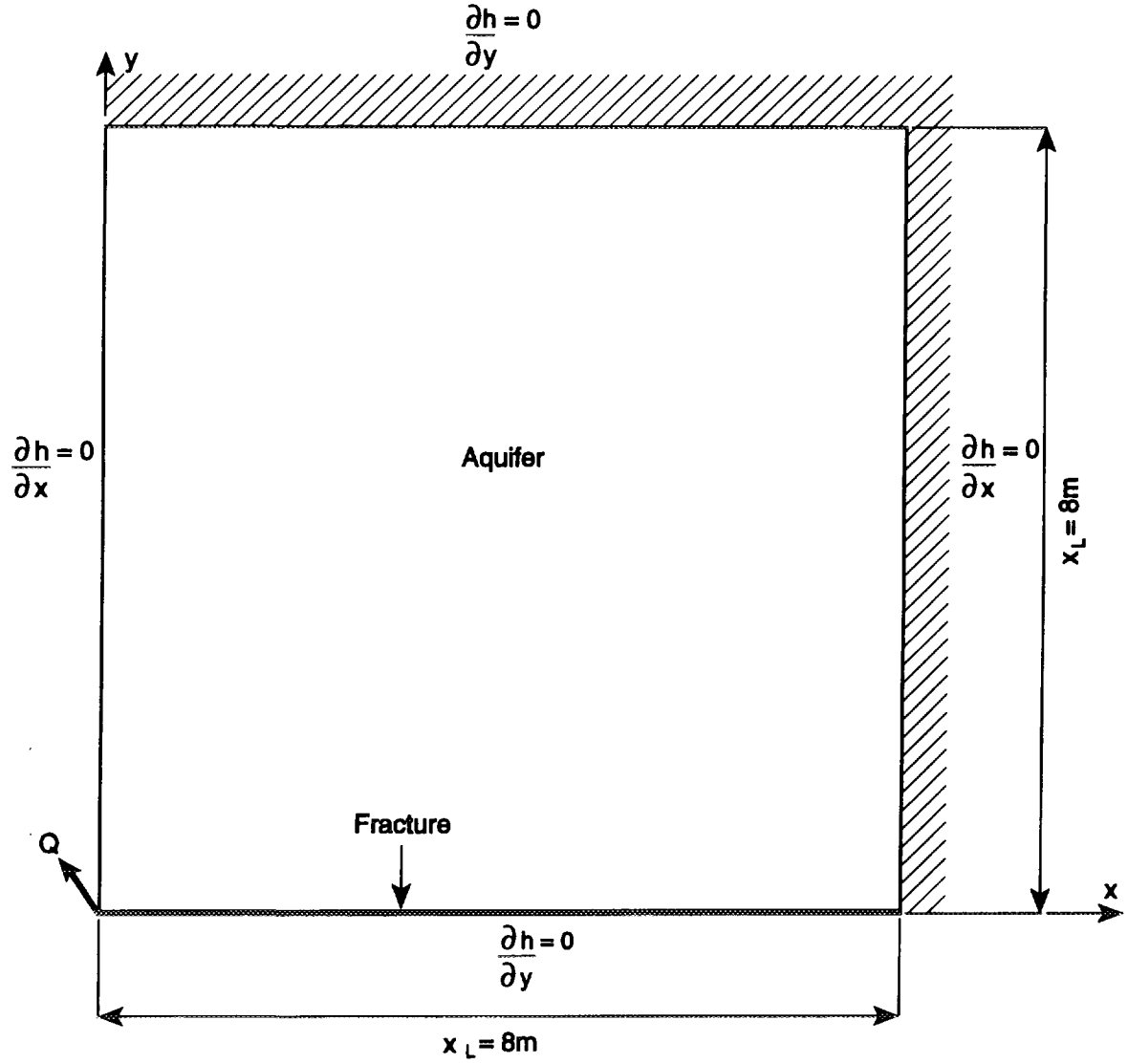

Spatial Discretization: 12 non-uniform increments;

in x direction starting at x = 0 for aquifer and fracture

Δx = 0.3, 0.4, 0.45, 0.6, 0.6, 0.65, 0.7, 0.8, 0.8, 0.8, 0.9, 1.0 m; and,

in y direction starting at y = 0 for aquifer

Δy = 0.1, 0.2, 0.3, 0.4, 0.5, 0.65, 0.75, 0.75, 0.85, 1.0, 1.0, 1.5 m

FIGURE 4: Case 2: Model Geometry, Boundary Conditions and MOTIF Spatial Discretization

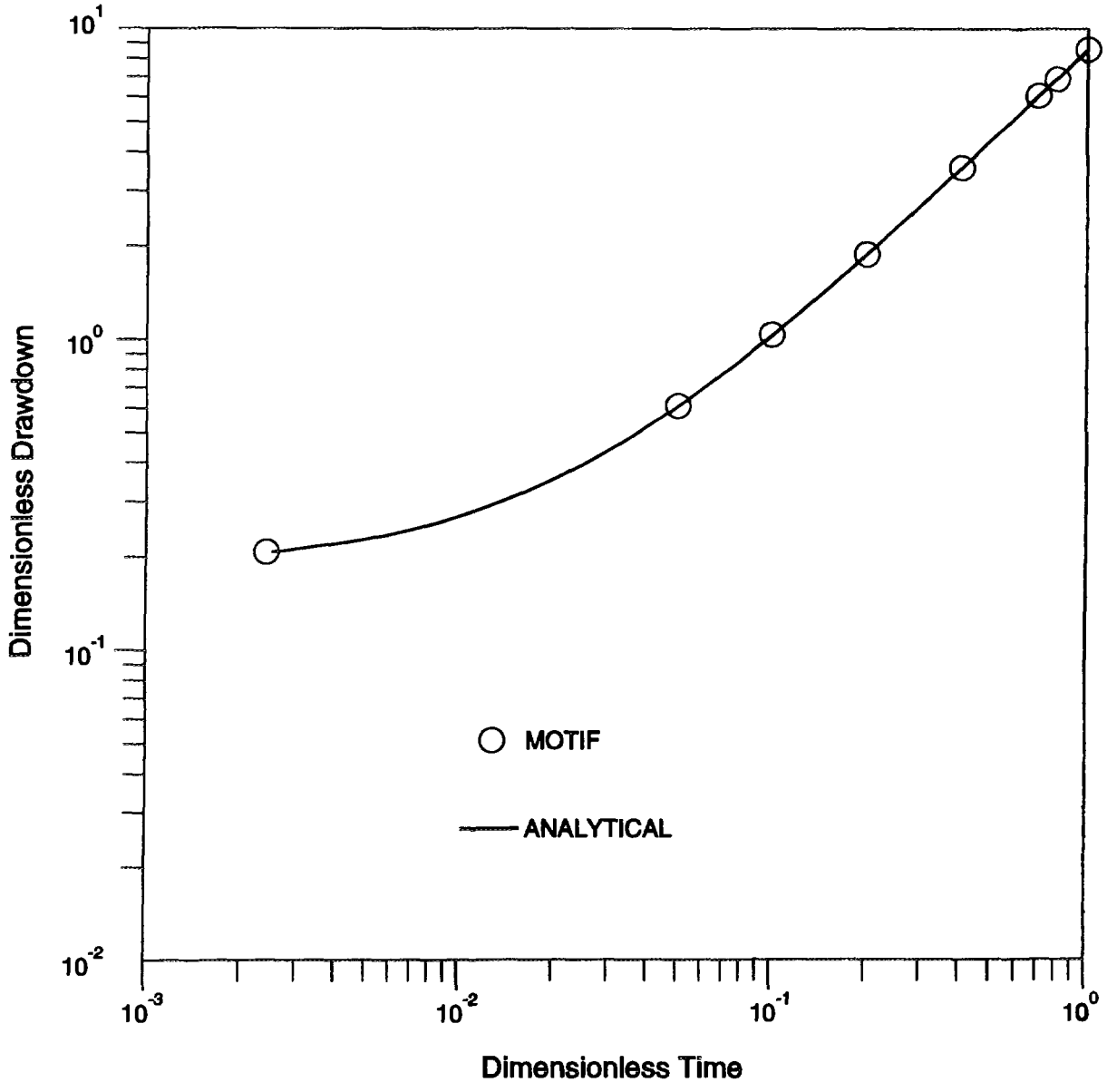

FIGURE 5: Case 2: Dimensionless Drawdown at the Withdrawal Well Versus Dimensionless Time

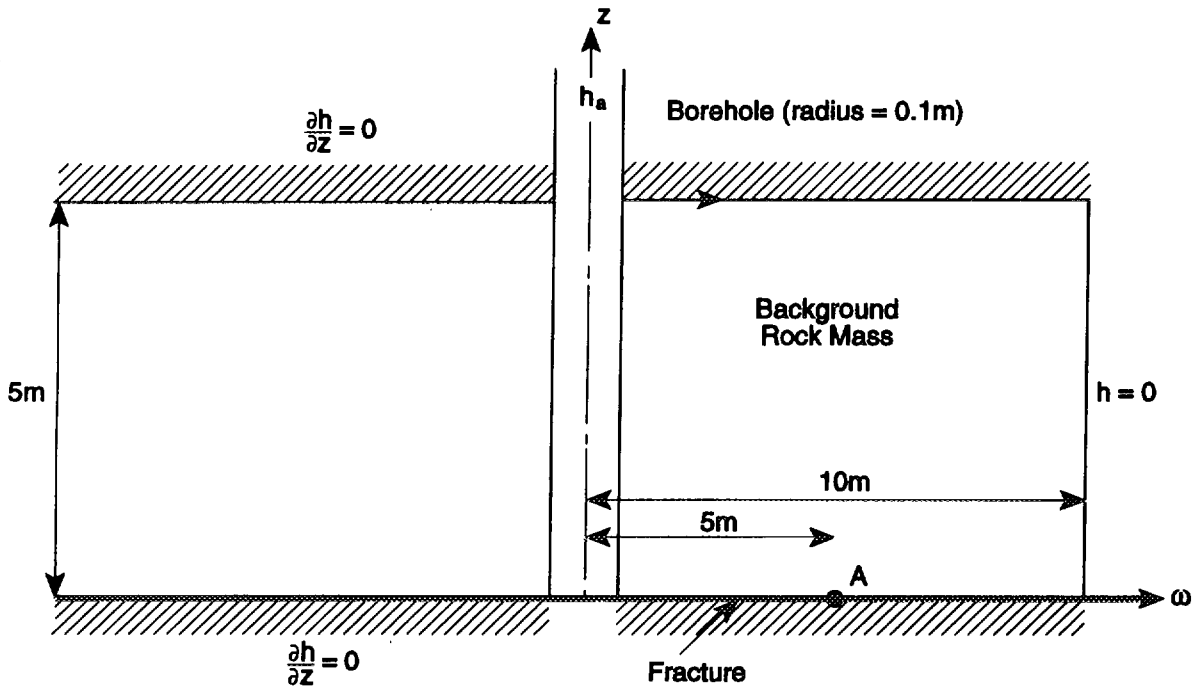

FIGURE 6: Case 3: Model Geometry and Boundary Conditions

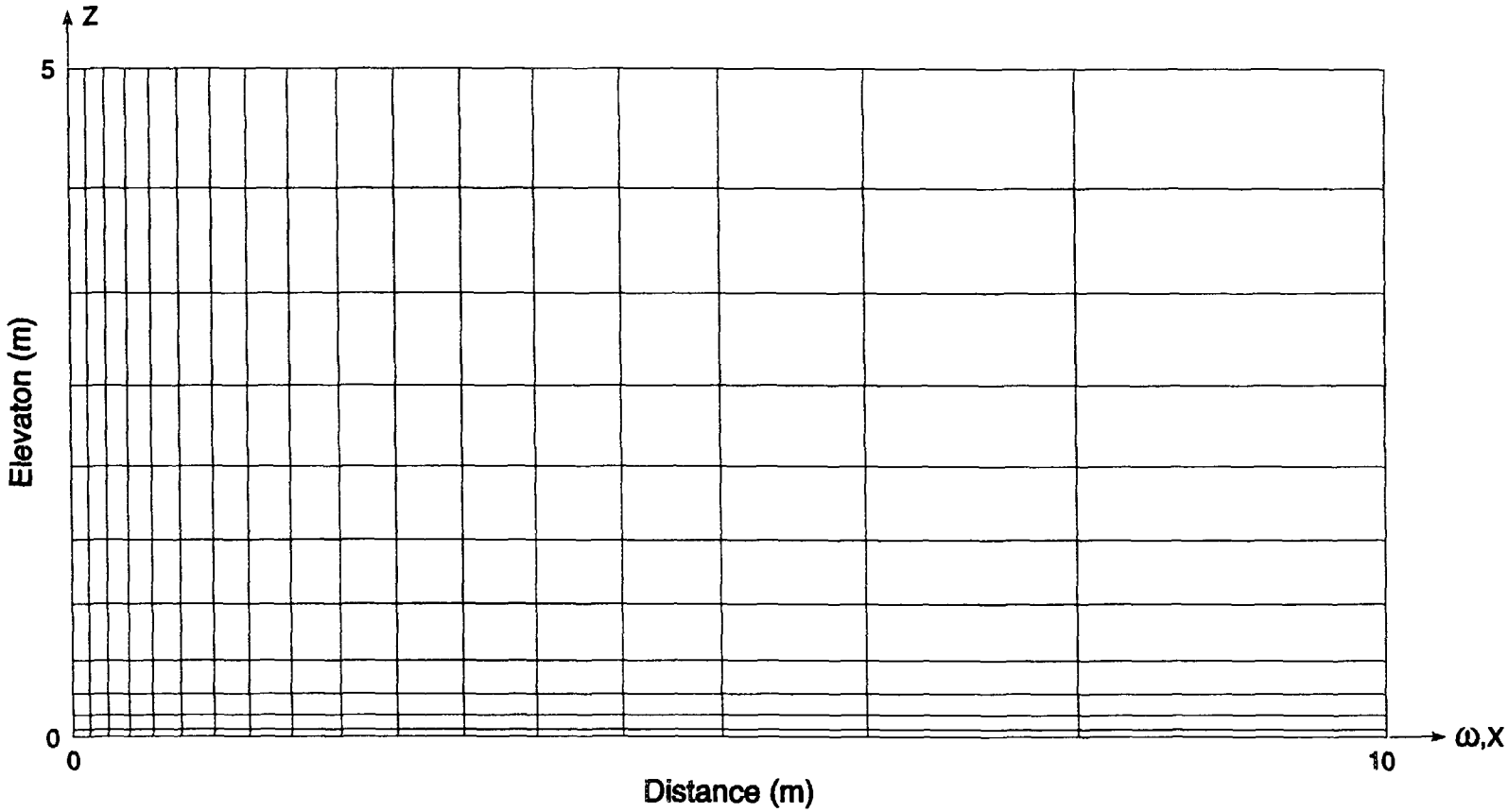

FIGURE 7: Case 3: MOTIF Spatial Discretization

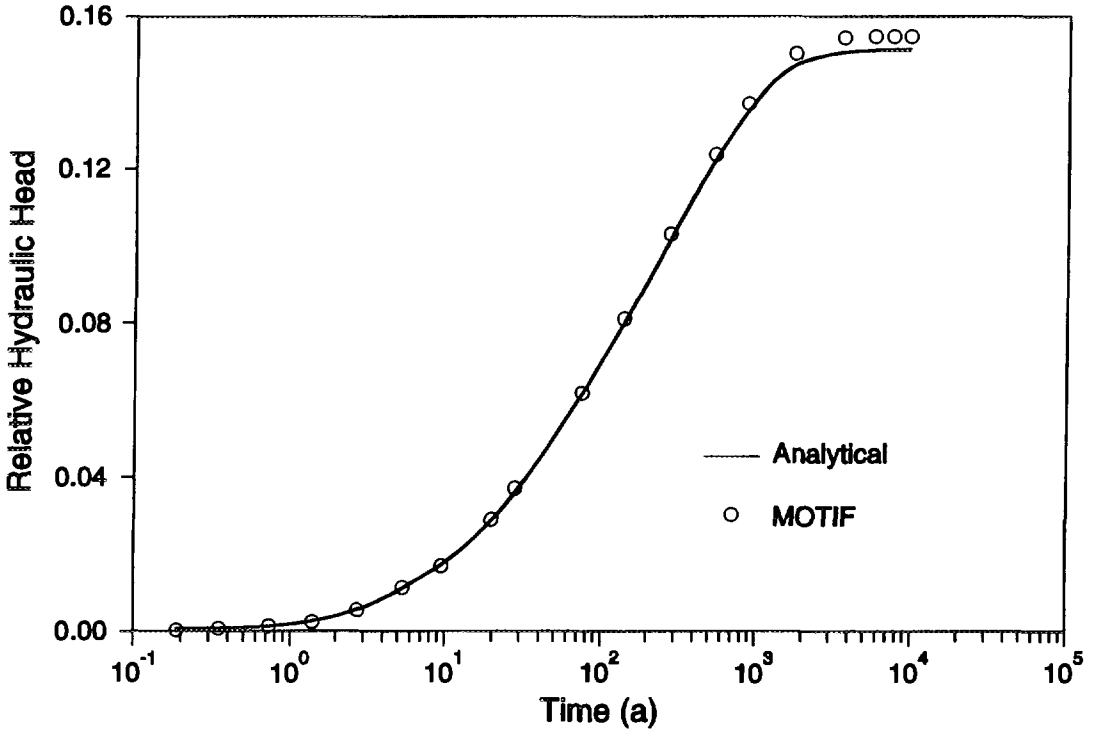

FIGURE 8: Case 3: Relative Hydraulic Head at Point A in Fracture Versus Time

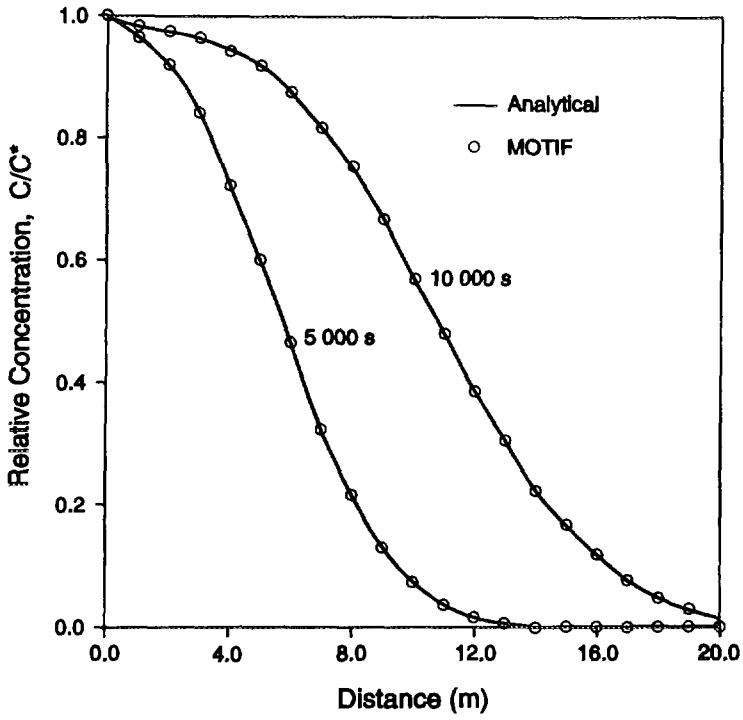

FIGURE 9: Case 4a: Relative Concentration Profiles at Various Times. Case includes advection and dispersion.

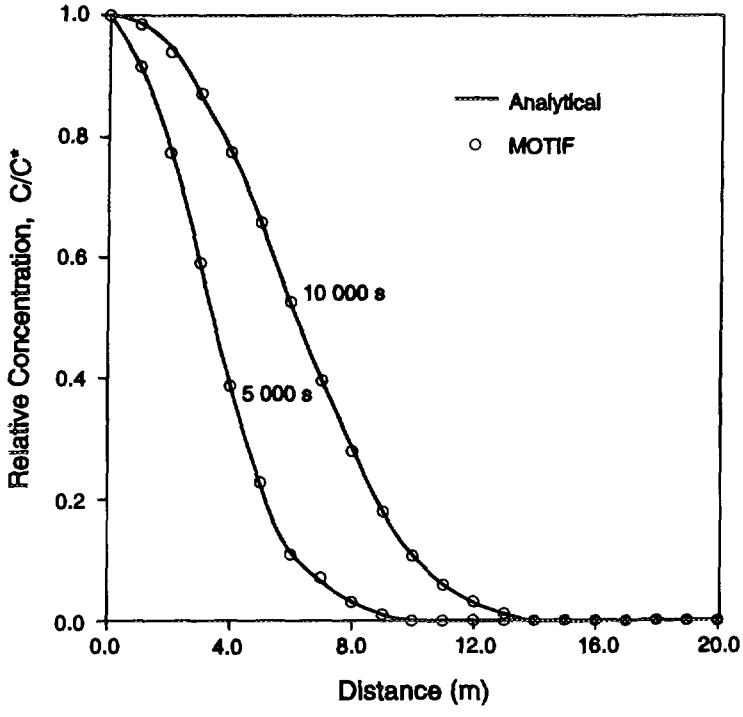

FIGURE 10: Case 4b: Relative Concentration Profiles at Various Times. Case includes advection, dispersion and linear equilibrium sorption.

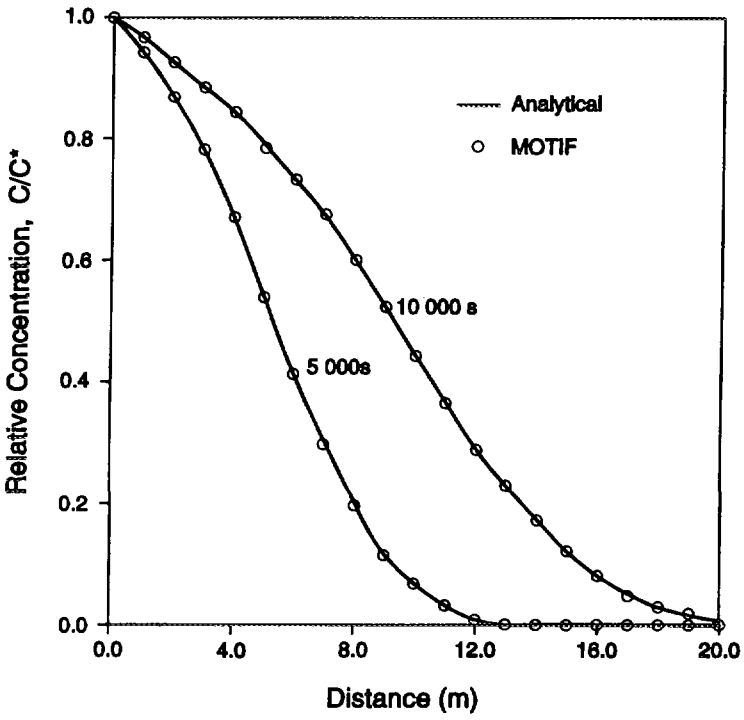

FIGURE 11: Case 4c: Relative Concentration Profiles at Various Times. Case includes advection, dispersion and radioactive decay.

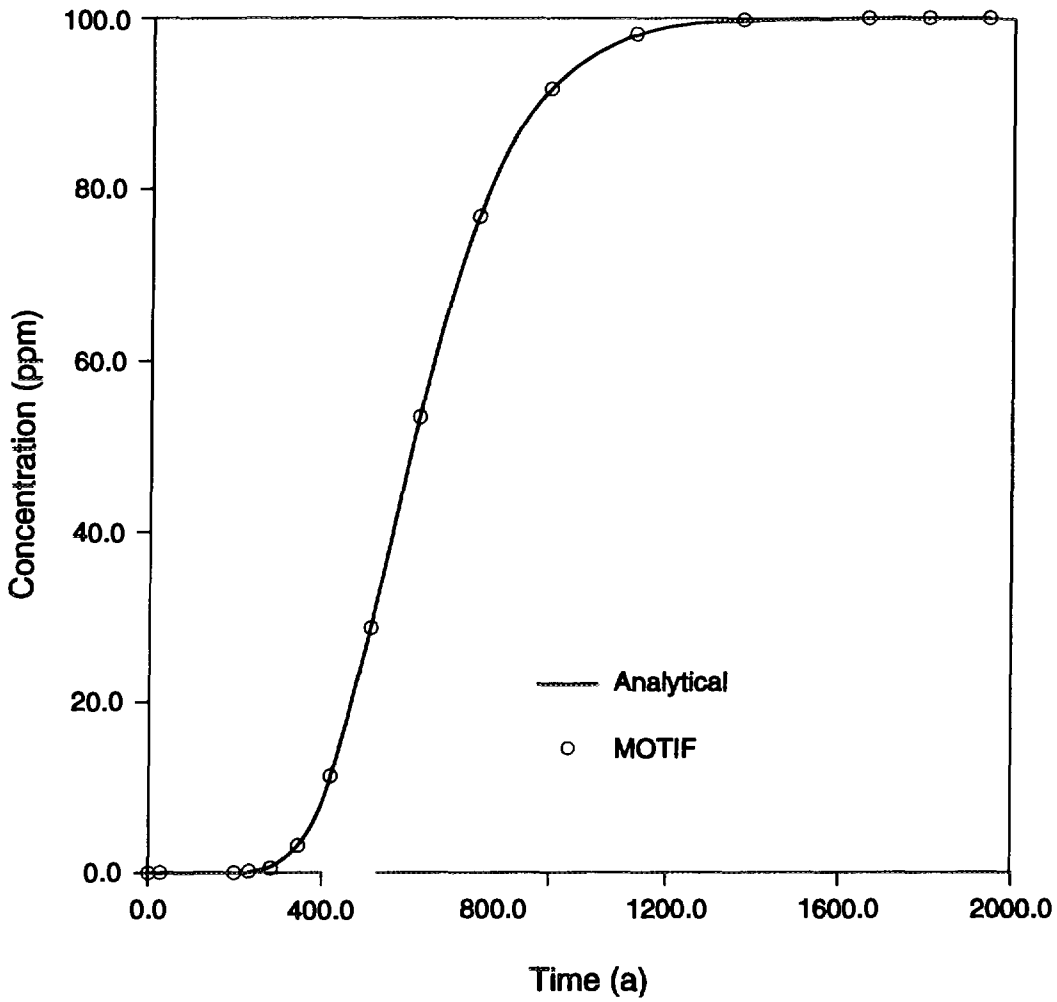

FIGURE 12: Case 5: Column Effluent Concentrations Versus Time

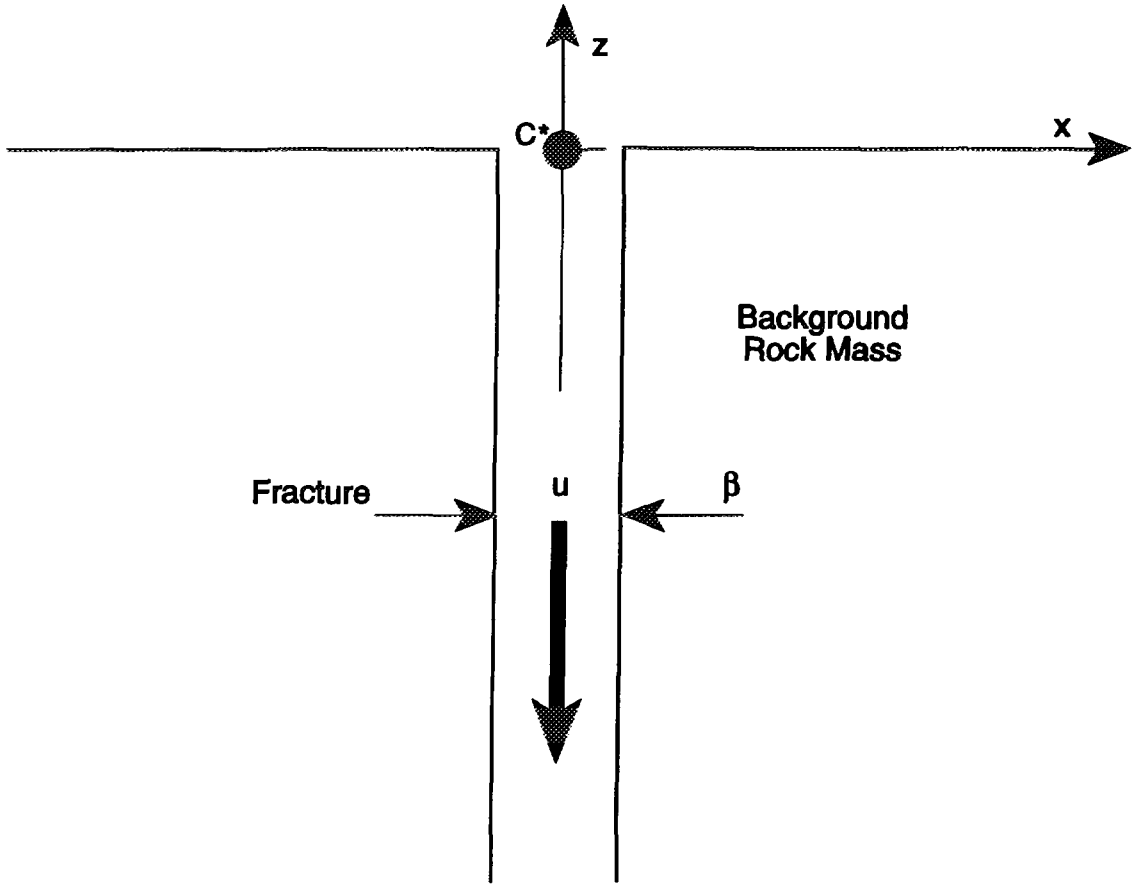

FIGURE 13: Case 6: Model Geometry

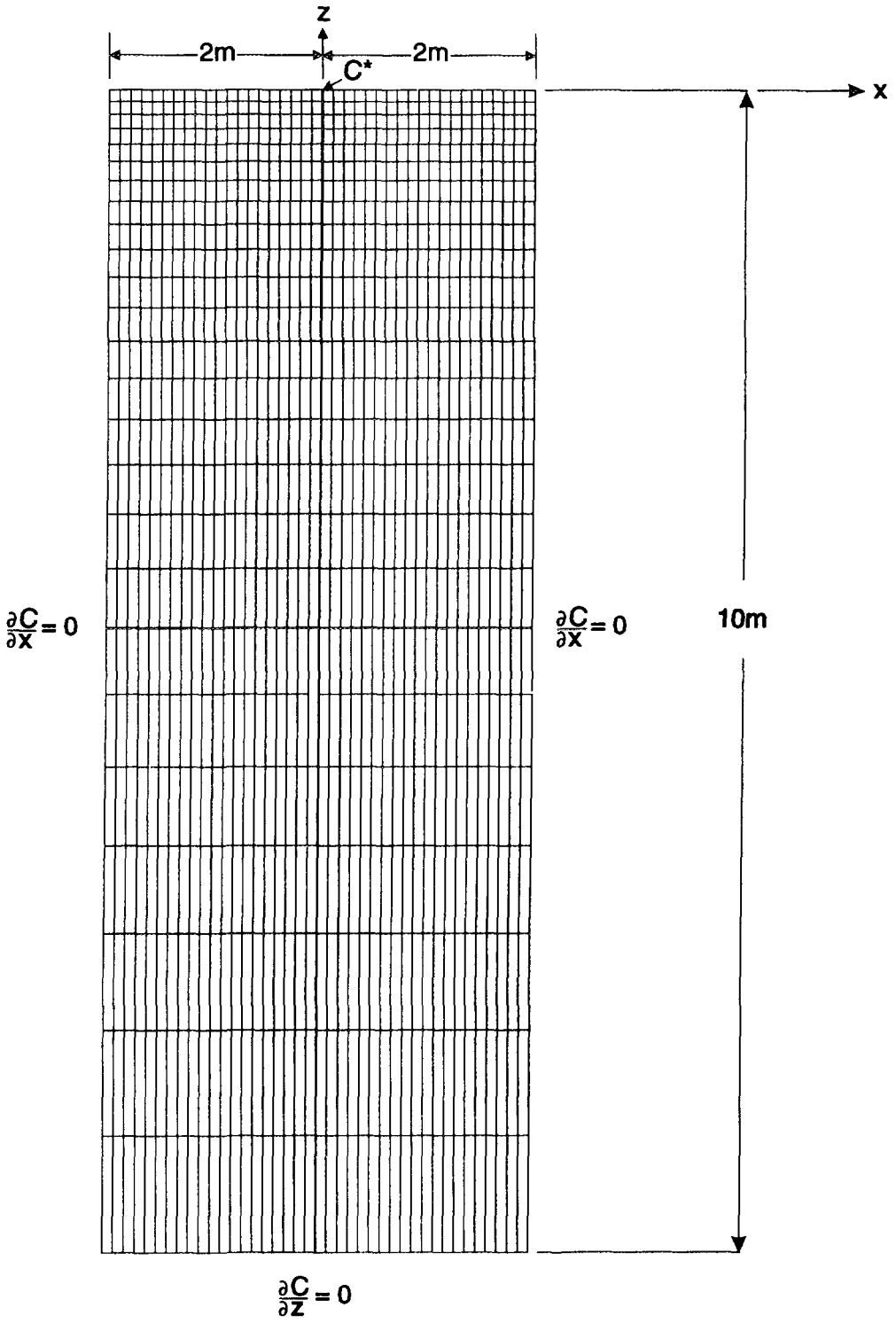

FIGURE 14: Case 6: MOTIF Spatial Discretization

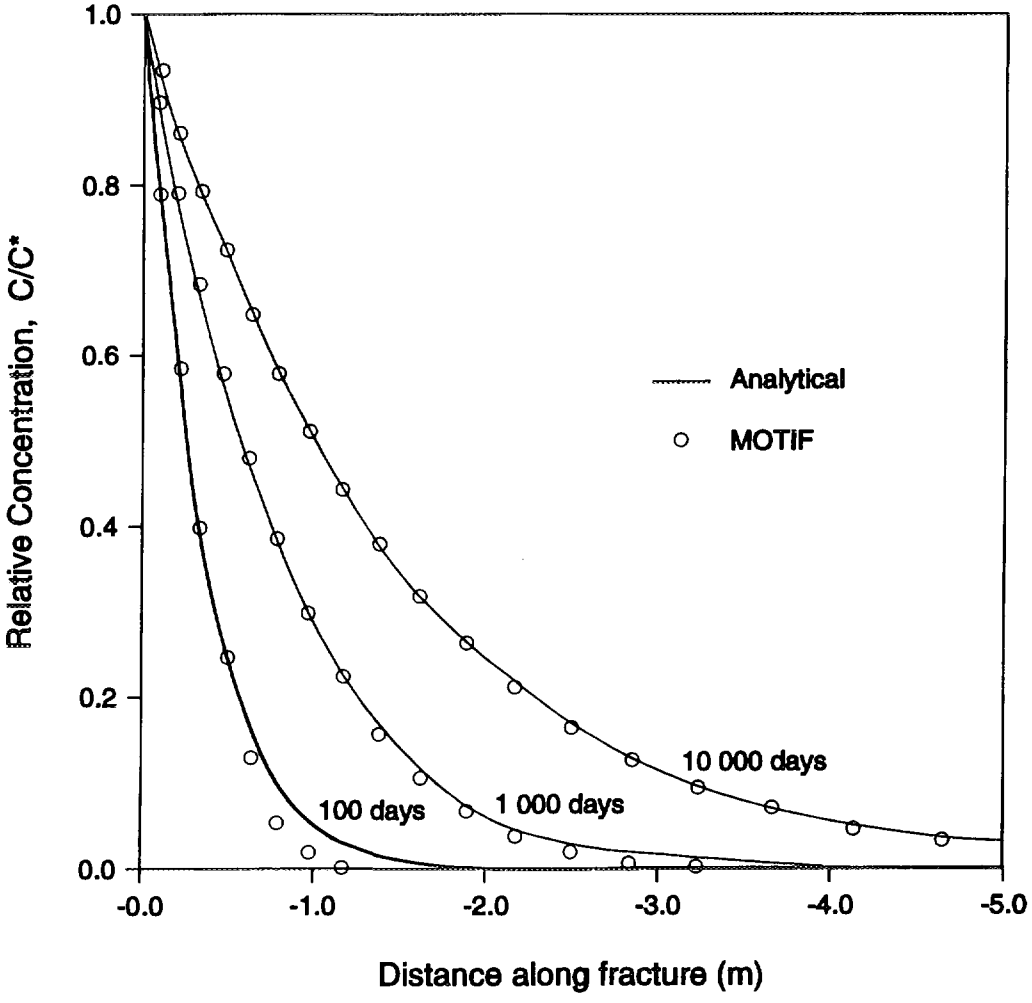

FIGURE 15: Case 6: Relative Concentration Profiles in the Fracture at Various Times

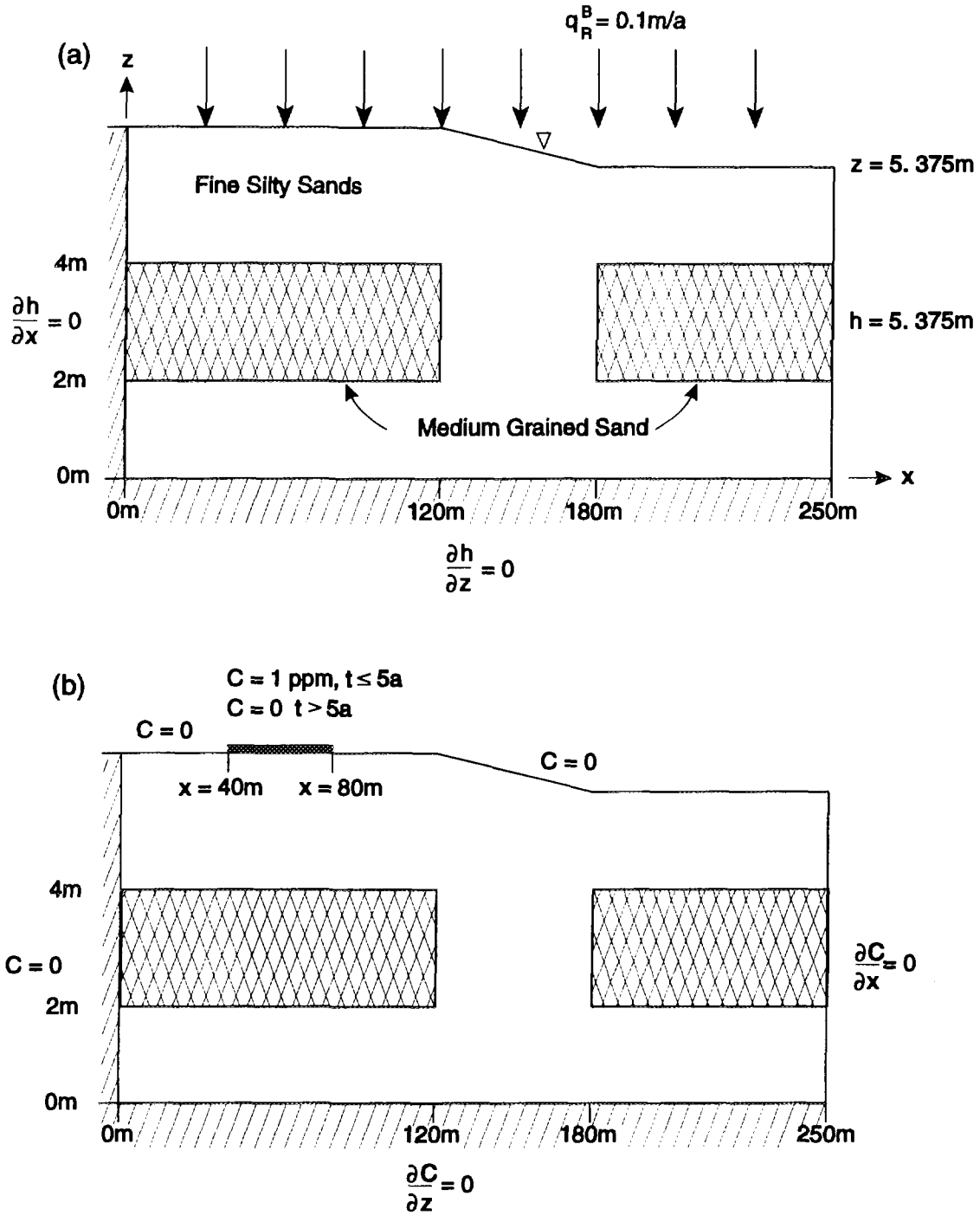

FIGURE 16: Case 7: Model Geometry and (a) Groundwater Flow Boundary Conditions, (b) Solute Transport Boundary Conditions

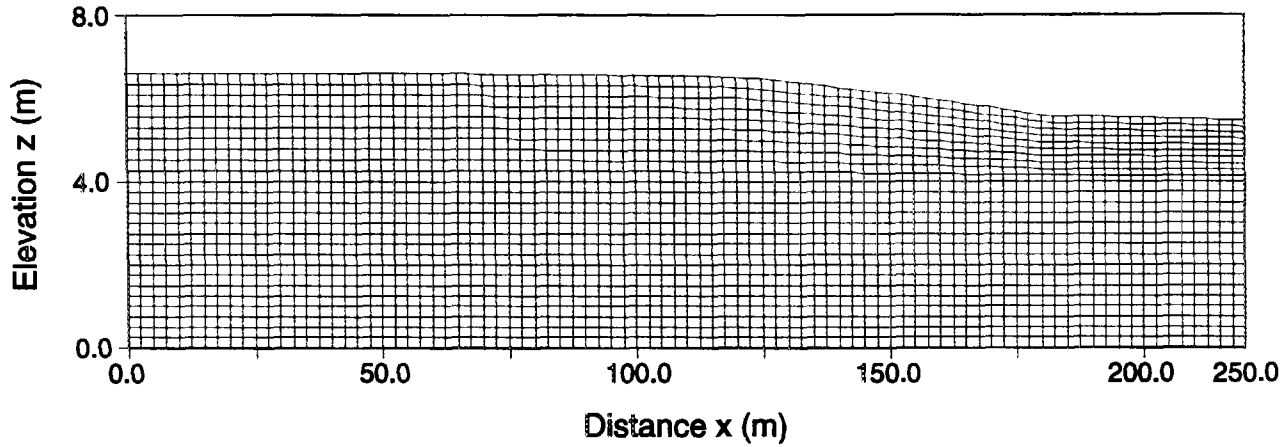

FIGURE 17: Case 7: MOTIF Spatial Discretization

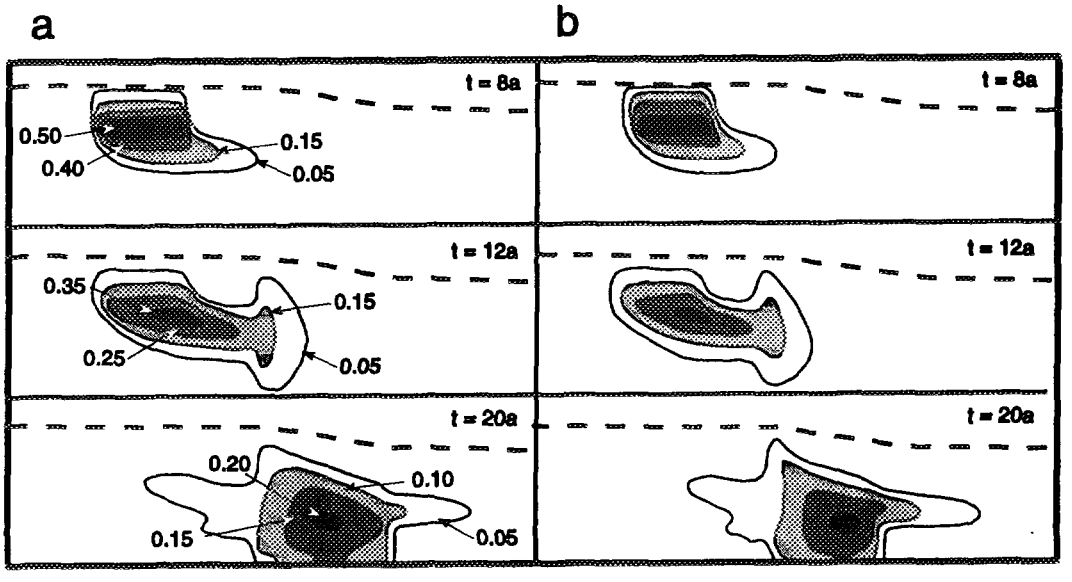

FIGURE 18: Case 7: Concentration Distributions (ppm) at Various Times
(a) Using MOTIF; (b) by Sudicky (1989)

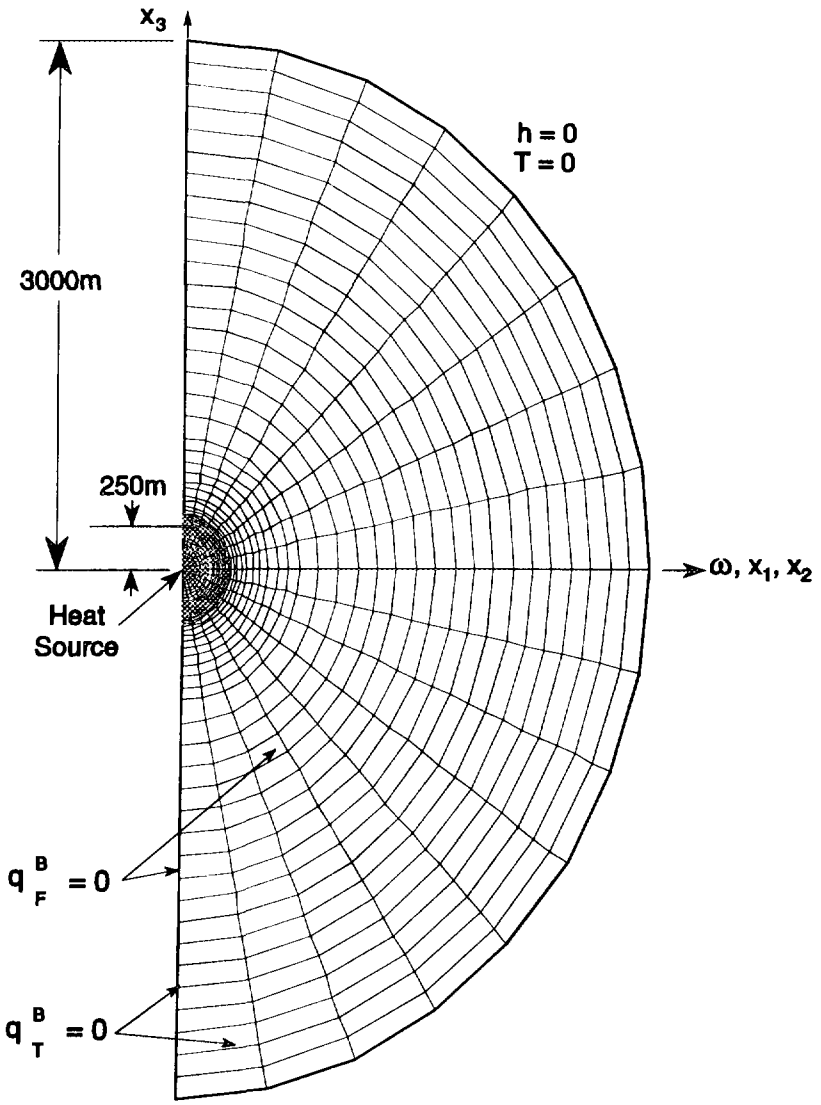

FIGURE 19: Case 8: MOTIF Spatial Discretization and Boundary Conditions

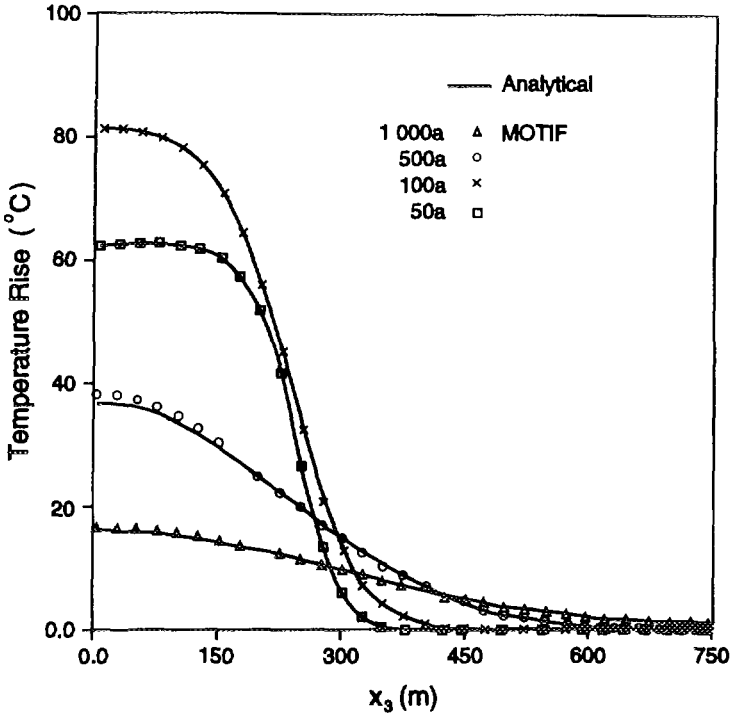

FIGURE 20: Case 8: Temperature Rise at Various Times as a Function of Vertical Distance (x_3) Above the Centre of the Heat Source

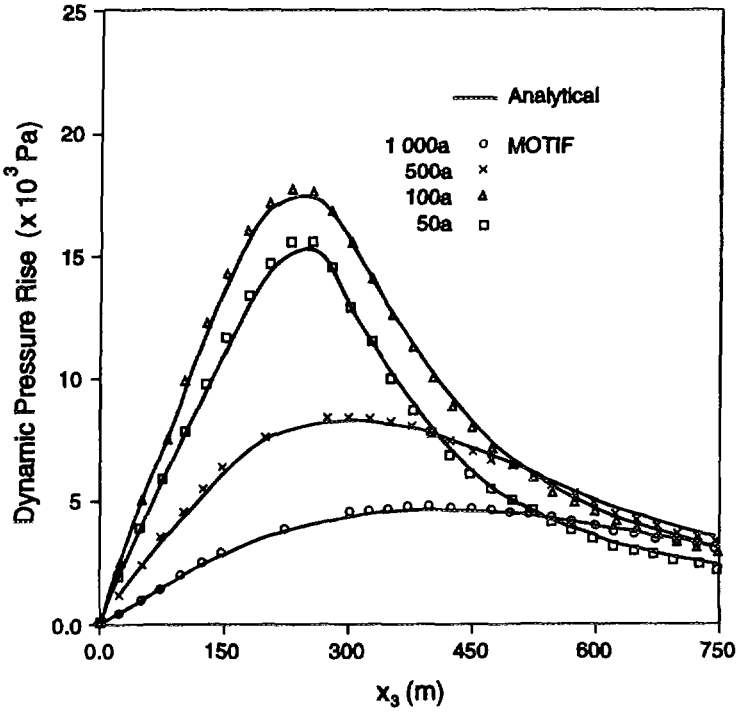

FIGURE 21: Case 8: Dynamic Pressure Rise at Various Times as a Function of Vertical Distance (x_3) Above the Centre of the Heat Source

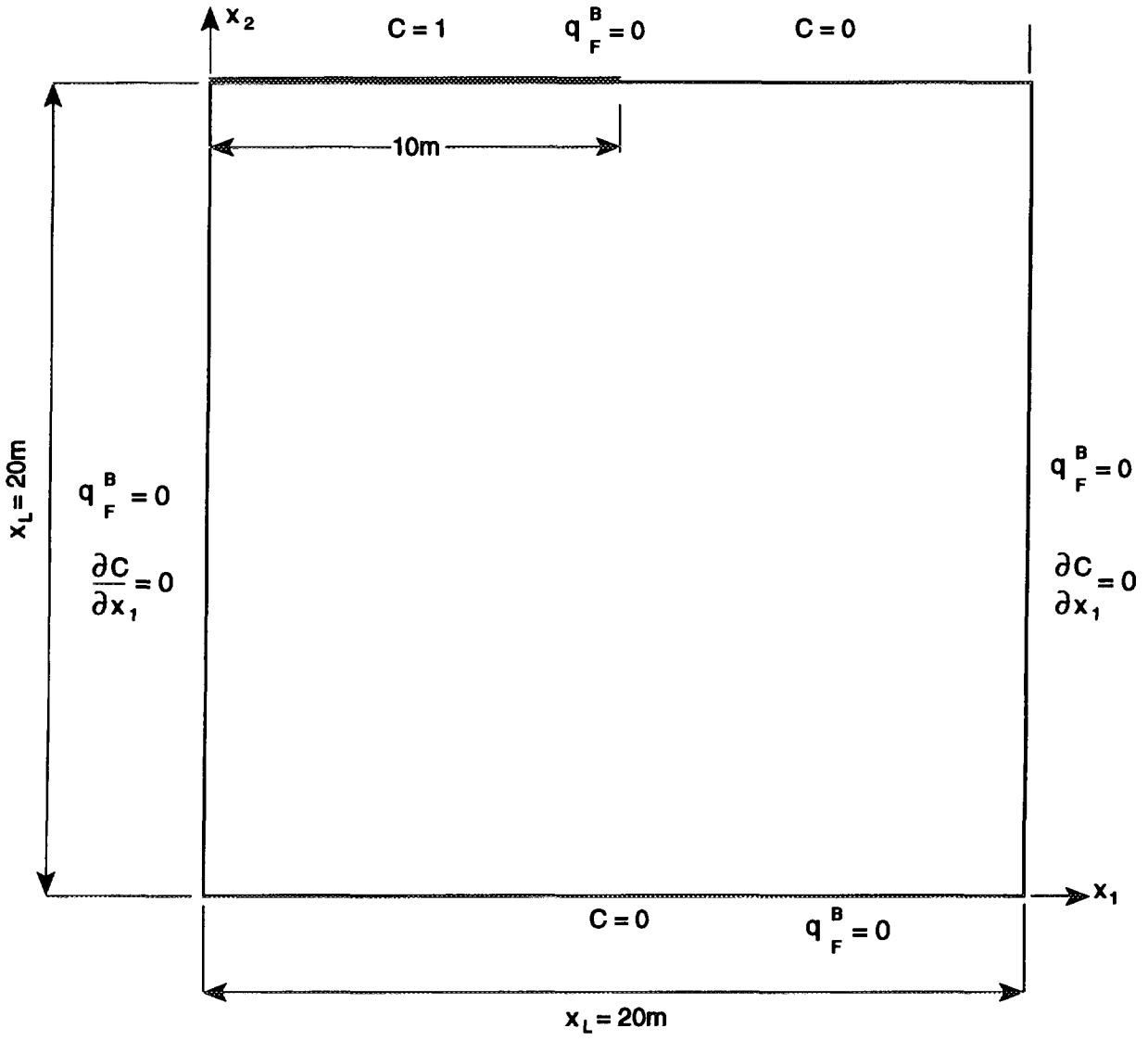

FIGURE 22: Case 9: Model Geometry and Boundary Conditions

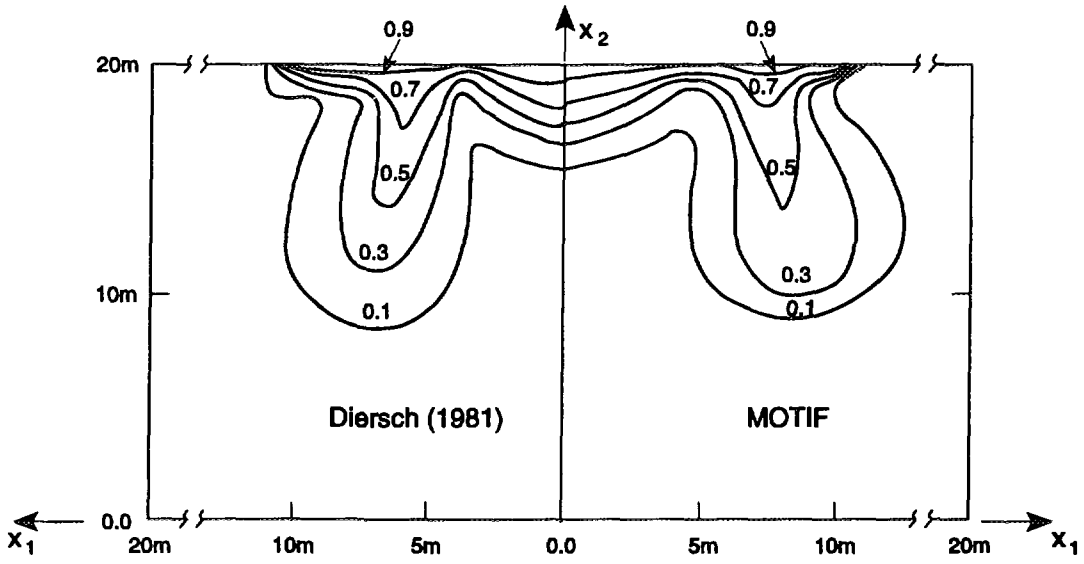

FIGURE 23: Case 9: Concentration Contours at Dimensionless Time of 0.01

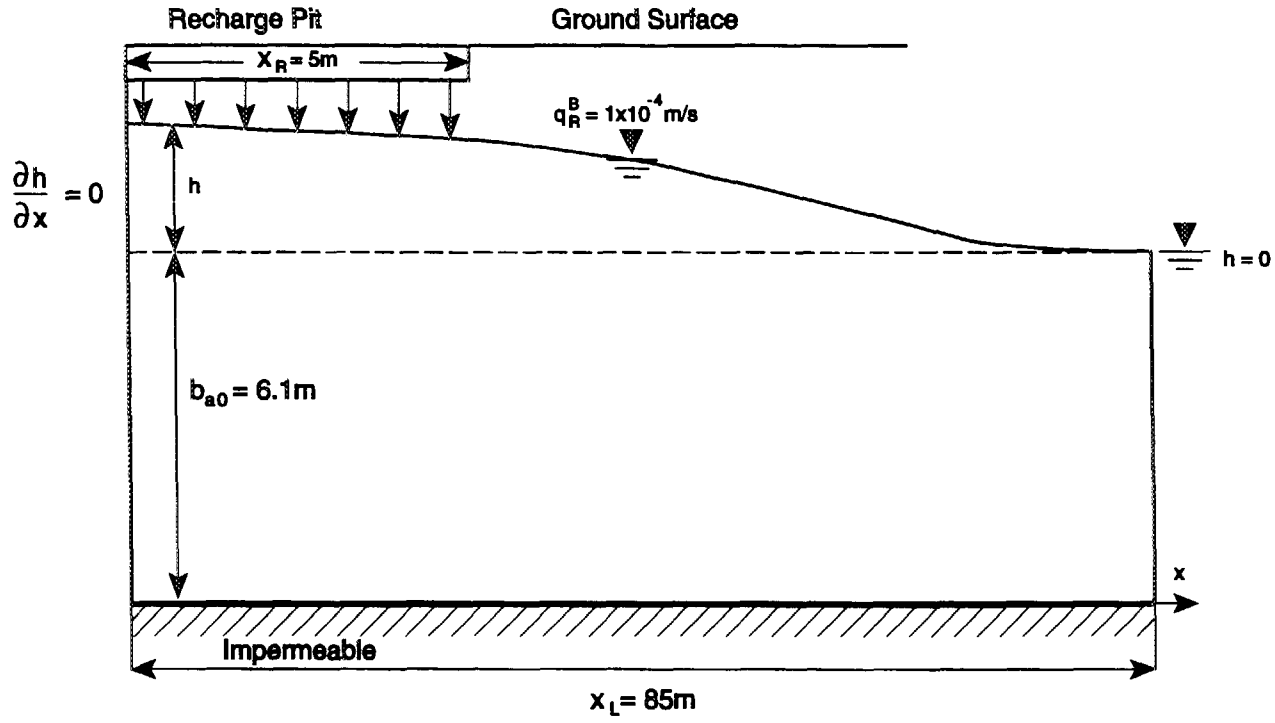

FIGURE 24: Case 10: Model Geometry and Boundary Conditions

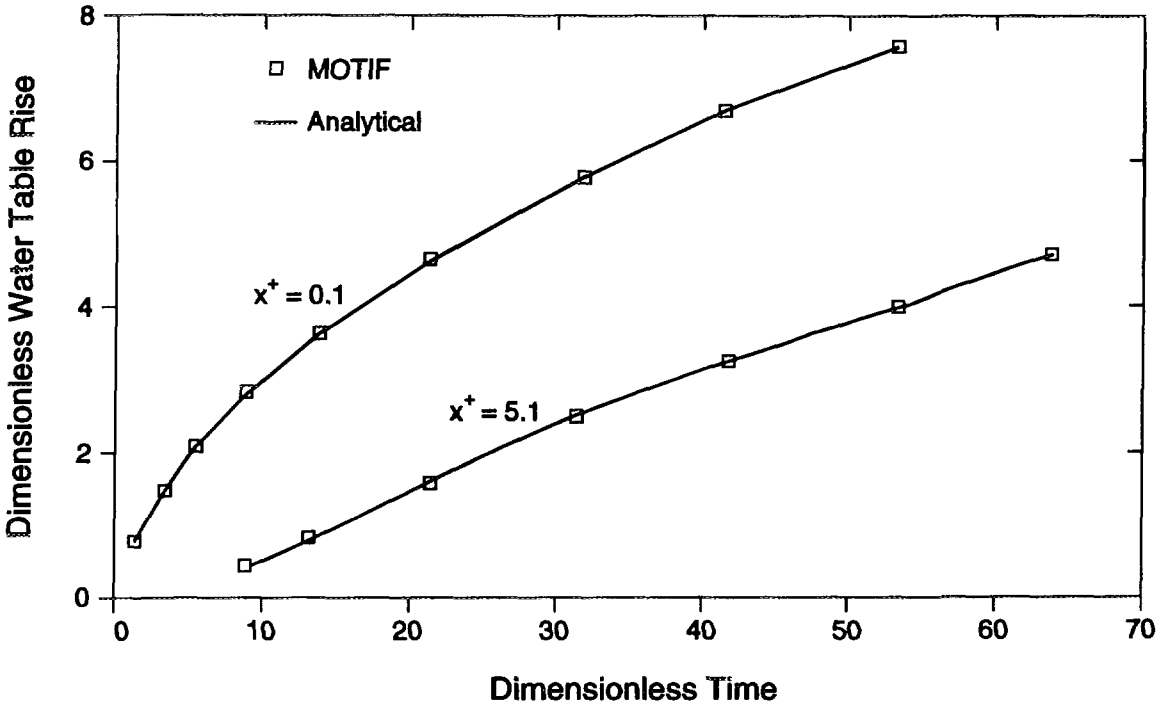

FIGURE 25: Case 10: Dimensionless Water Table Rise Versus Dimensionless Time at Dimensionless Distances of 0.1 and 5.1

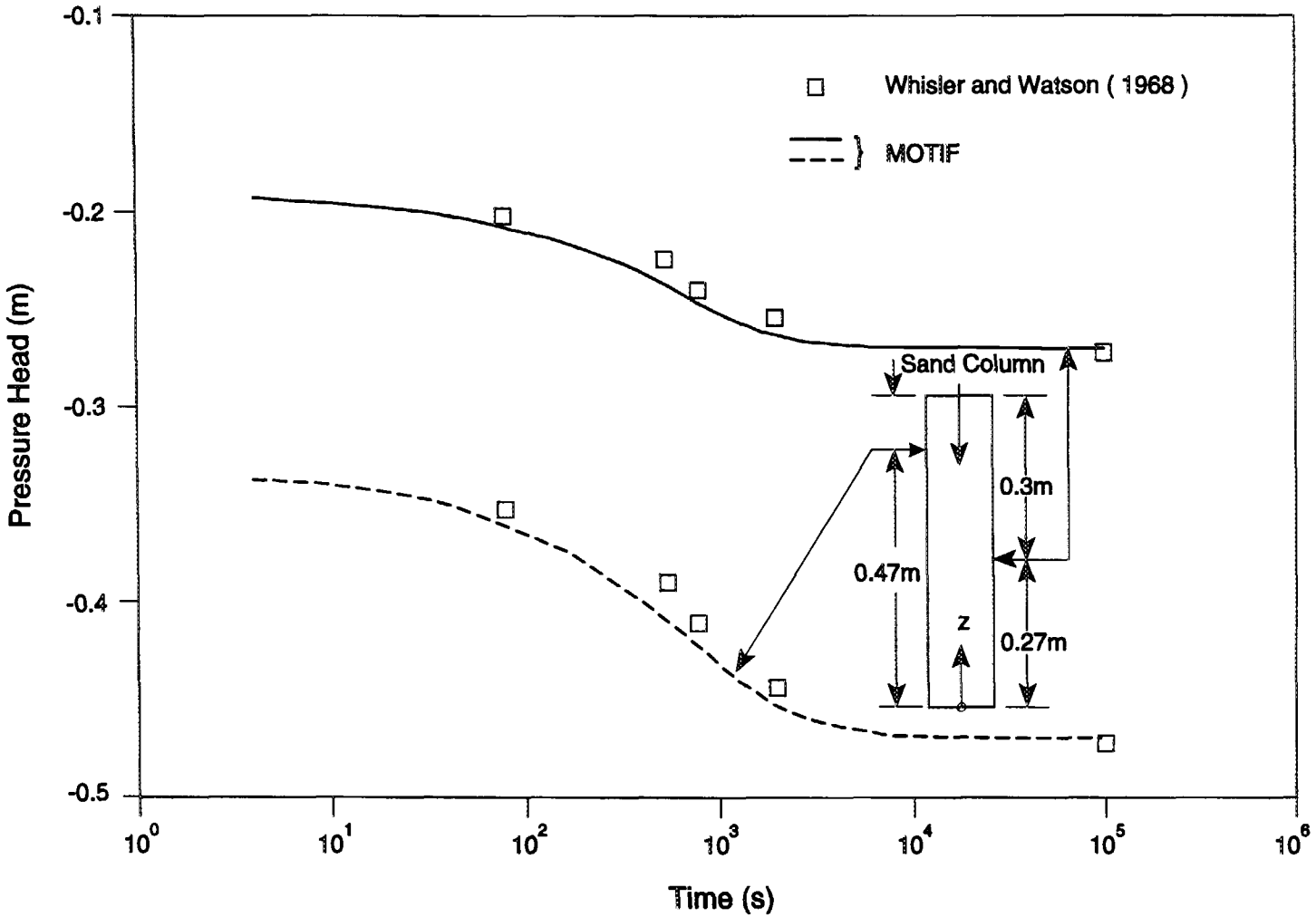

FIGURE 26: Case 11: Model Geometry and Pressure Head Versus Time at z = 0.27m and z = 0.47m

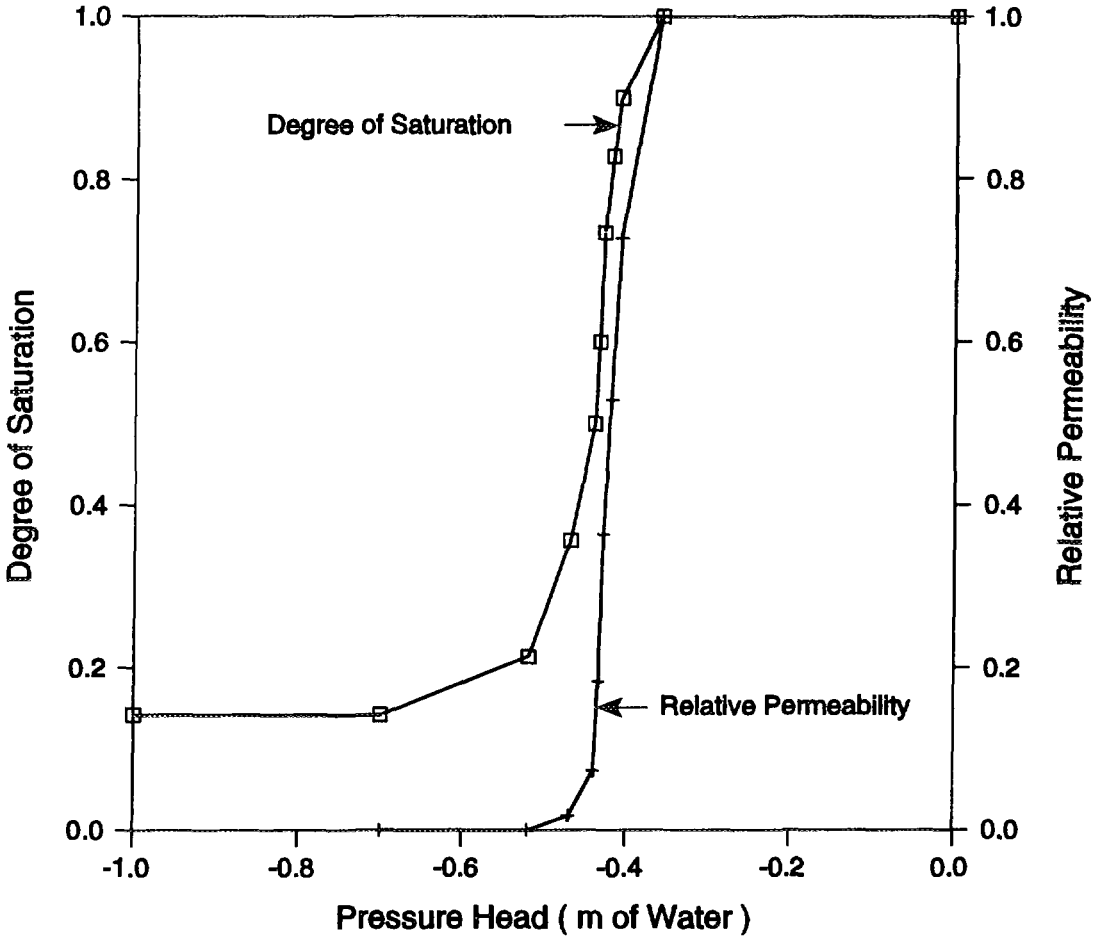

FIGURE 27: Case 11: Characteristic Curves for the Drainage of Water from the Sand

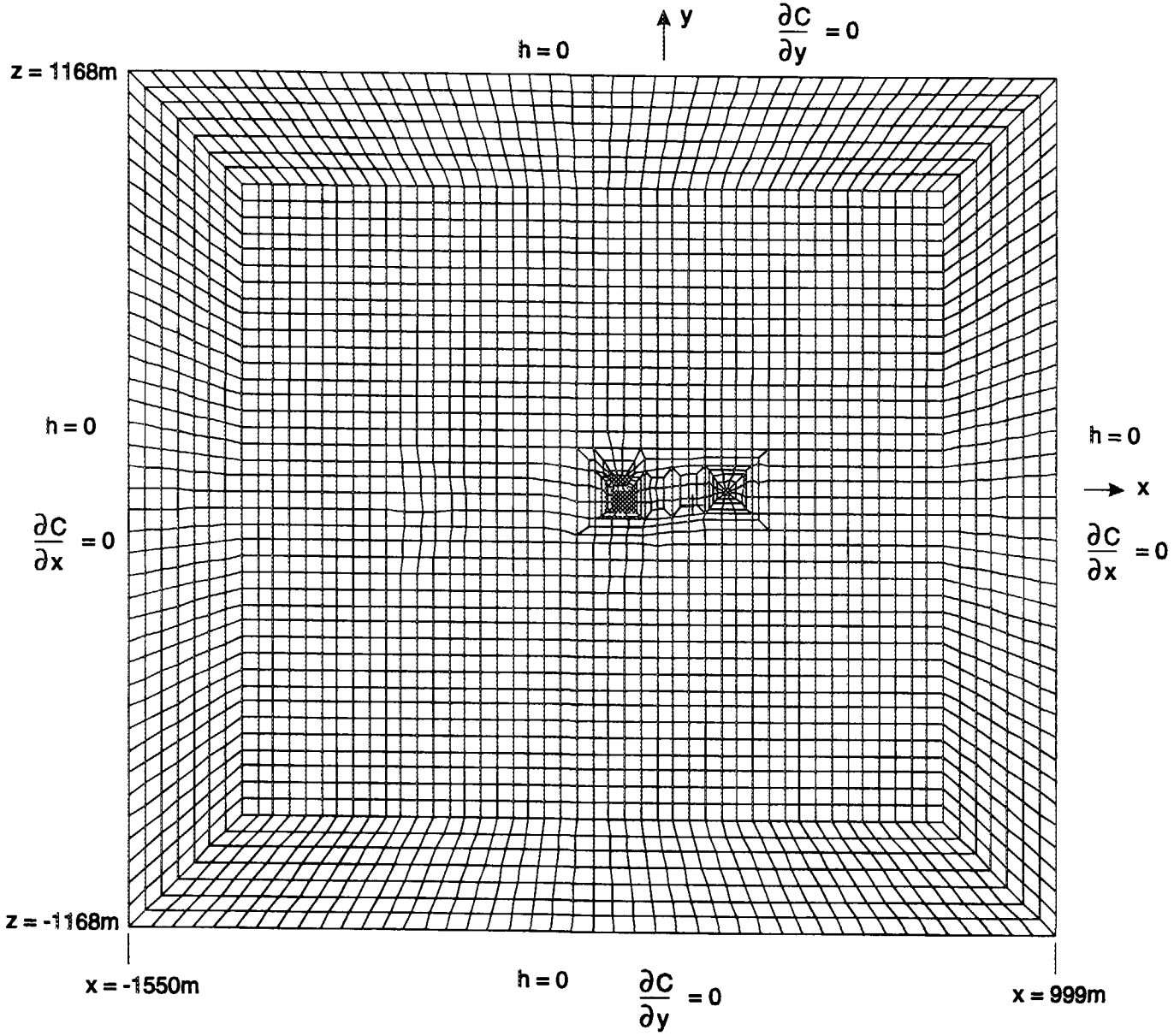

FIGURE 28: Case 12 & 13: MOTIF Spatial Discretization and Boundary Conditions

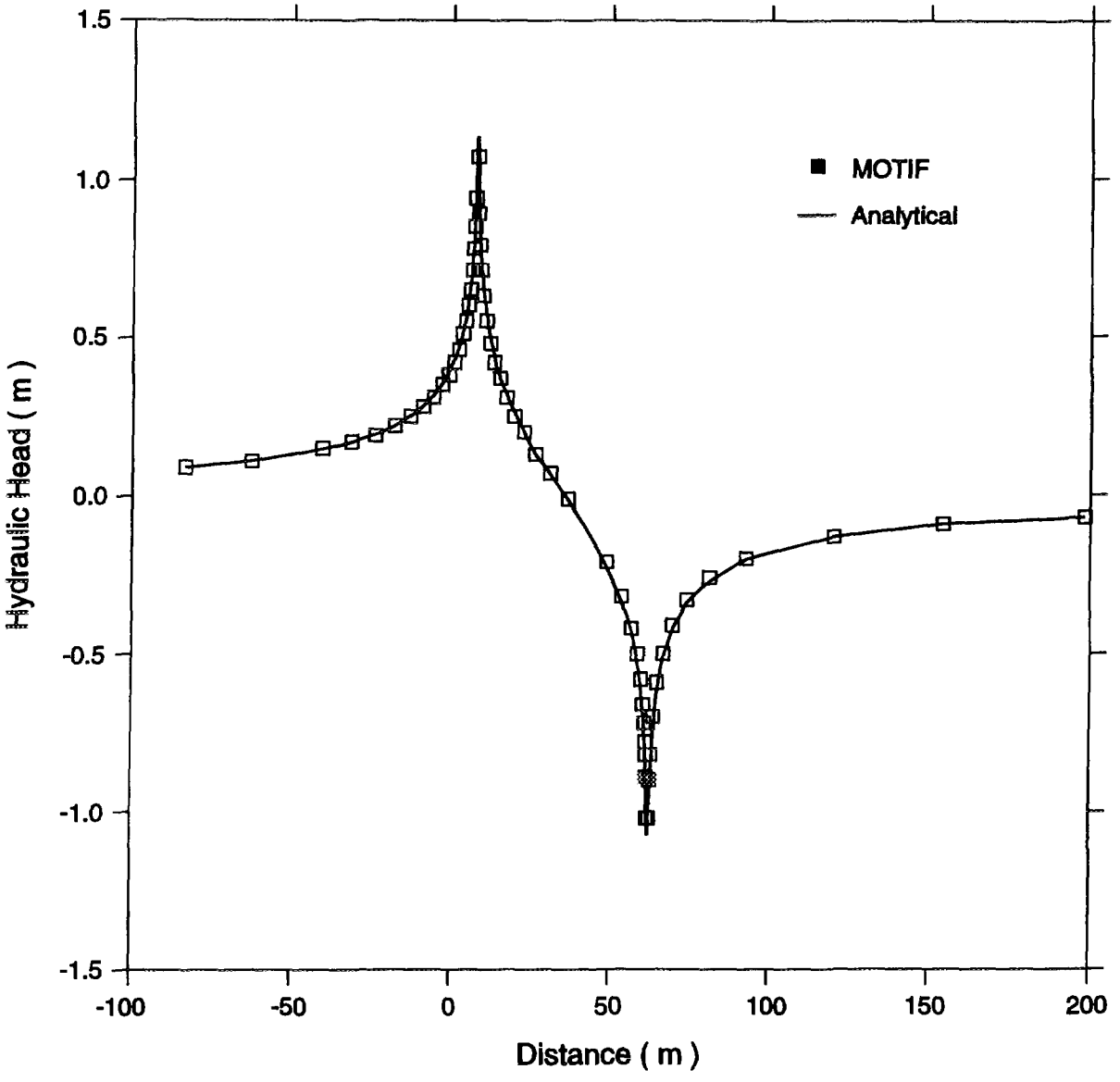

FIGURE 29: Case 12: Hydraulic Head Along the Line Passing Through the Injection and Withdrawal Wells

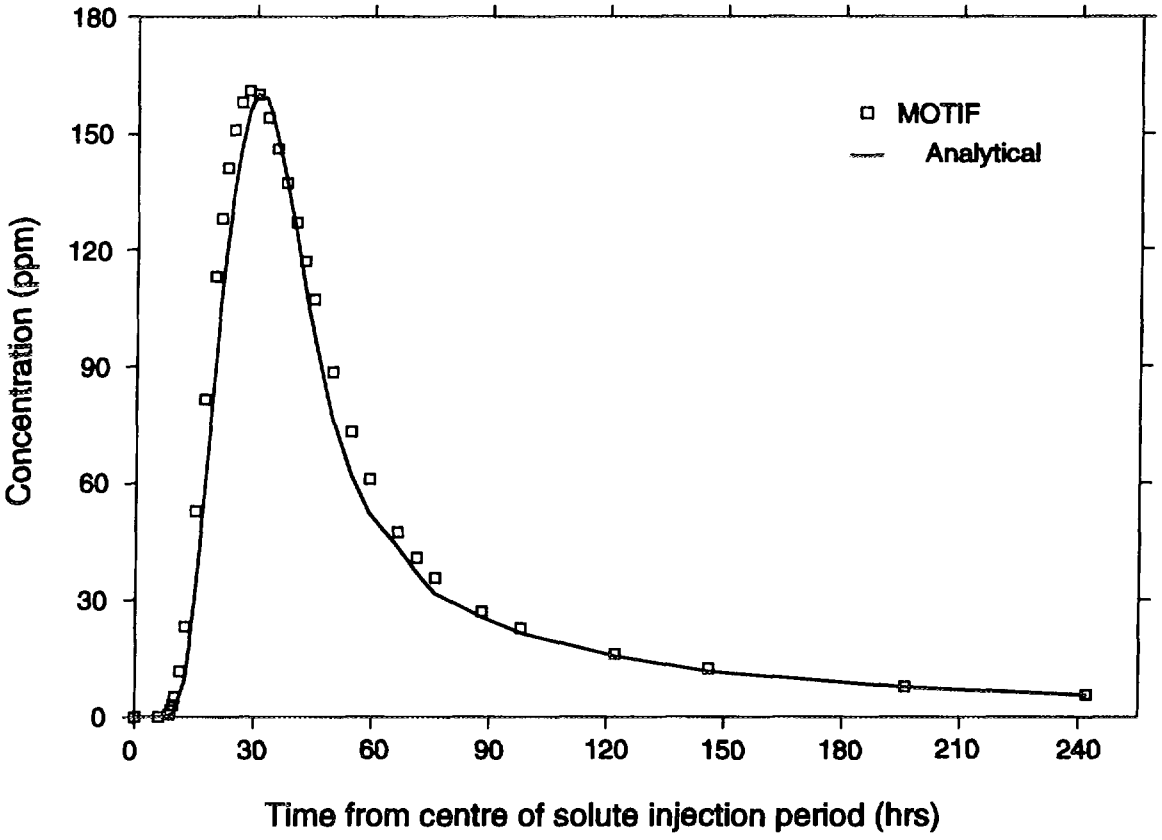

FIGURE 30: Case 13: Solute Concentration at the Withdrawal Well Versus Time

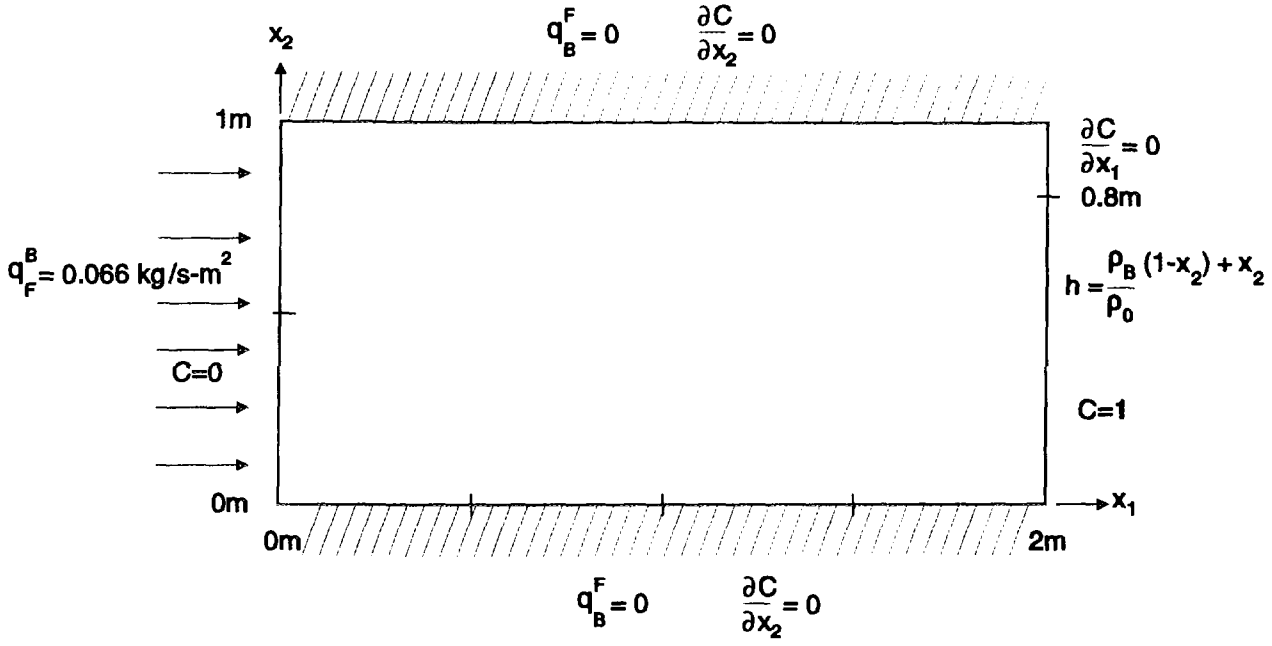

FIGURE 31: Case 14: Model Geometry and Boundary Conditions

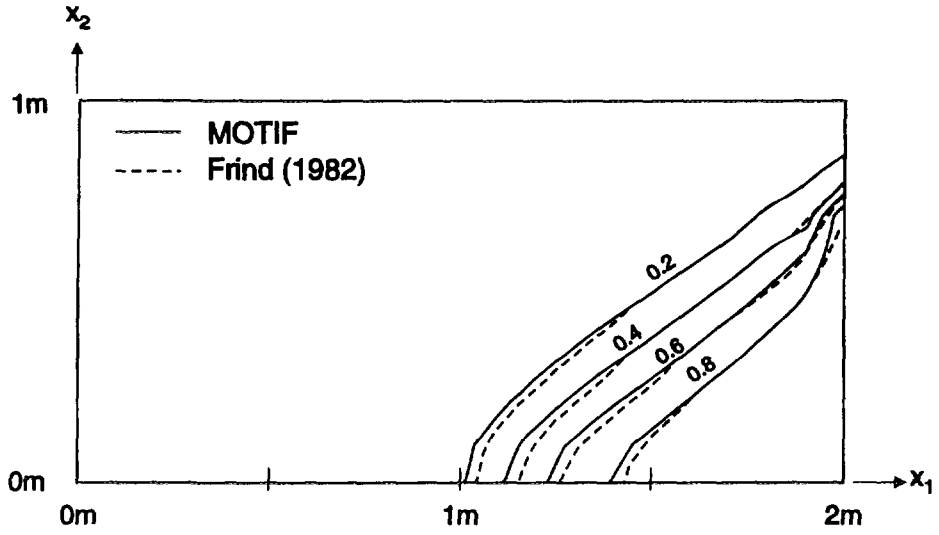

FIGURE 32: Case 14: Equilibrium Solute Concentration Contours

Cat. No. / Nº de cat.: CC2-11496E
ISBN 0-660-16714-X
ISSN 0067-0367

To identify individual documents in the series, we have assigned an AECL- number to each. Please refer to the AECL- number when requesting additional copies of this document from

Scientific Document Distribution Office (SDDO)
AECL
Chalk River, Ontario
Canada K0J 1J0

Fax: (613) 584-1745 Tel.: (613) 584-3311
ext. 4623

Price: B

Pour identifier les rapports individuels faisant partie de cette série, nous avons affecté un numéro AECL- à chacun d'eux. Veuillez indiquer le numéro AECL- lorsque vous demandez d'autres exemplaires de ce rapport au

Service de Distribution des documents officiels (SDDO)
EACL
Chalk River (Ontario)
Canada K0J 1J0

Fax: (613) 584-1745 Tél.: (613) 584-3311
poste 4623

Prix: B